ACIT5930
MASTER THESIS
in
Applied Computer and Information Technology (ACIT)

May 2023

Applied Artificial Intelligence

Design and Development of a Bio-Inspired Flying Drone

Alexander Halseth

Department of Computer Science
Faculty of Technology, Art and Design

OSLOMET

Preface

This thesis documents the design and development of a bio-inspired drone with a focus on morphing wing capabilities. The project was inspired by the flight capabilities of smaller birds that can adapt to their surrounding to increase their maneuverability in harsh environments. The goal was to explore these capabilities on a larger scale while also considering the possibility of scaling it down in the future.

With a growing interest in new and innovative technology and a bachelor's degree in drone technology from the University of Tromsø, this thesis ticked every box I was searching for in an engaging master's thesis. It allowed me to apply my previously acquired knowledge in addition to gaining insight into new methods and techniques in a relatively new field of research.

Oslo, May 15th 2023

Acknowledgments

First and foremost, I want to thank my supervisor, Vahid Hassani, for his support, encouragement, and guidance throughout this project.

I would also like to thank my fellow students for their comradery throughout this journey. A special mention goes to Aksel Johan Frafjord, Jan-Philip Radicke, and Pierre Boniface, who created an amazing work environment filled with engaging questions and insightful answers. Their willingness to help and share knowledge has been priceless in this project.

Lastly, I would like to thank my family and friends for their support and continuous encouragement throughout the duration of this project.

Abstract

This thesis presents the design, development, and testing of a bio-inspired drone with morphing wing capabilities to enhance flight performance and versatility by mimicking the adaptability of natural fliers. The research methodology comprises an iterative design, prototyping, and testing process to explore different morphing wing mechanisms and building materials to optimize such a system.

An initial morphing mechanism involving a cogwheel-based system evolved into a sliding rack system to efficiently reduce the wing area of a fixed-wing drone. Throughout its development, the drone's fragility posed a challenge due to multiple crashes during test flights. However, these tests provided insight into the performance and flight characteristics of the drone and underscored the importance of a sufficiently planned operation. The fourth test flight demonstrated the effective operation of the morphing mechanism during flight, enabling the drone to roll in both directions by reducing the wing area on the opposite side.

In the end, this project demonstrated the potential of utilizing morphing wing capabilities for fixed-wing drones and provided a possible application for use in micro drones, where they could be able to adapt to their environment and withstand challenging conditions. The research laid a foundation for the future development of similar drones. Furthermore, future improvements that could optimize and enhance the drone's performance are discussed to continue the development of a drone inspired by nature's most adept fliers.

Contents

List of Figures

List of Tables

Chapter 1

Introduction

This chapter will present the motivation behind this problem statement and briefly introduce some concepts related to morphing wings. In the end, the problem statement will be described, and a plan for how to explore and find a suitable solution will be presented.

1.1 Motivation

Nature has long been a source of inspiration for humankind, pushing us towards pursuing new techniques and ideas. Two examples of how nature has directly inspired technological advances are the humpback whale fins and the maple seed. The fins from the humpback whale inspired the design of a biomimetic fin that, based on simulations, reduces drag and increases lift for aircraft, watercraft, and windmills [14]. The descent of the maple seed served as an inspiration for the Samurai Unmanned Aerial Vehicle (UAV), developed by Lockheed Martin. This UAV is just a wing with a propeller attached, and it achieves lift similarly to how a maple seed spins around while descending.

Concepts found in nature have not only been an inspiration for new designs, but it has also been a source of inspiration for innovative techniques and methodologies. Artificial intelligence has adopted many concepts from nature, such as the artificial neural network, genetic algorithms, and swarm intelligence [25].

Nature has been fundamental in the development of flight. Birds and other airborne creatures have inspired humans to pursue the ability to fly, and since the Wright brothers took flight in 1903, more advances have been made. One of these advances stems from the bird's adaptability in changing its wing shapes, sizes, and rotation according to its current task.

Morphing wings refer to the ability to transform the shape of an aircraft's wings. This ability to change the shape, size, or angle of the wing during flight can increase the performance of an aircraft during various conditions and can prove particularly useful for UAVs, especially small UAVs [1]. Being able to morph its wings during flight can increase the maximum payload, reduce take-off and landing distances, and increase flight time by increasing fuel efficiency for UAVs [1].

Most commercial UAVs have an upper limit on the wing speed for safe operations, a problem that affects smaller UAVs more due to their lower weight and reduced power. Smaller UAVs could take advantage of the wind if they could transform their wings to adapt to the environment. However, designing and producing a UAV capable of morphing its wings while maintaining good aerodynamics during the transformation poses challenges. The mechanical components required for the wing transformation could quickly exceed the maximum take-off weight, and the complexity of such a design on a smaller scale makes such UAVs challenging to manufacture. Furthermore, it could also remove some fundamental steering mechanics from fixed-wing drones, such as the ability to roll [8].

One of the earliest attempts to create a UAV with morphing wings is the Morphing Flight-Vehicle Experimental (MFX-1), a 100 lb jet-powered drone. The morphing of the wings was done by a single motor, which meant it could only morph the wings symmetrically during flight, and it was able to adjust the area of its wing by approximately 40%[15]. Other examples include the RoboSwift, which featured wings covered in carbon fiber feathers [27], and the Pigeonbot, which utilized artificial feathers for even more movement during the morphing [7]. Research has also been conducted to produce a drone capable of replicating a bird's flapping motion for propulsion, replacing the traditional propulsion method of a motor with a propeller [41].

This thesis will attempt to create a drone with morphing wing capabilities that can replace the ailerons used by conventional fixed-wing drones. This will be done by drawing inspiration from previous work in related fields to create a full-size fixed-wing drone with morphing capabilities that could be utilized for smaller UAVs.

1.2 Problem Statement

This thesis aims to design and develop a bio-inspired drone to explore the potential for scaling down the technology for use in micro-drones. The project will investigate bio-inspired designs, such as morphing wing capabilities, and attempt to apply these concepts in a full-size drone.

The goal is to address the challenges in designing, manufacturing, and controlling a bio-inspired drone while maintaining maneuverability and some degree of aerodynamics. The final product should demonstrate the possibility of incorporating a bio-inspired concept on a drone and will be evaluated based on the viability of adapting this technology.

Chapter 2

Background and Related Work

This chapter will provide a historical overview and a literature review of morphing wings, flapping wing micro air vehicles, and drones. In addition, several fundamental concepts related to drones and their design and development will also be explained.

2.1 Morphing wings

Morphing wing refers to the ability to change a wing's shape during flight and has been in use ever since the Wright Brothers first took to the air in 1903. Their aircraft featured cables that were attached to the wings, allowing them to twist the wings during flight so that the plane could perform a roll action. Throughout time, numerous different versions of morphing wings have been developed.

In 1994 NASA initiated the Smart Structures Morphing Program, which looked into smart materials, adaptive structures, and optimization and controls to enhance the efficiency of air and space vehicles [24]. Subsequently, in 2002, the Defense Advanced Research Project Agency (DARPA) came up with a program to investigate morphing wings. In the first phase, they funded three companies that each adopted a different approach. Lockheed Martin began working with a shape memory polymer that could be folded when stimulated with an electric current [19]. The second company, NextGen, contributed with a fixed-wing in which the morphing was controlled by different control systems on the drone [15]. The third approach was developed by Raytheon Missile Systems, which developed morphing wings for a cruise missile instead of an aircraft [18].

There have been multiple attempts to develop UAVs with morphing wings. One example is the work of [8], where the skeletal structure of a bird's wing was used as inspiration for the design and development of the drone's wings. As illustrated in Figure 2.1, the outer parts of the wings are similar to that of a bird in the way that they can fold in. This prototype is able to reduce the total area of the wings by 41% when folded. Furthermore, when the wings are fully extended, the lift coefficient is increased by 32%. As was noted in the introduction, the wings of the drone are compromised of feathers, making it challenging to attach ailerons that can assist it in

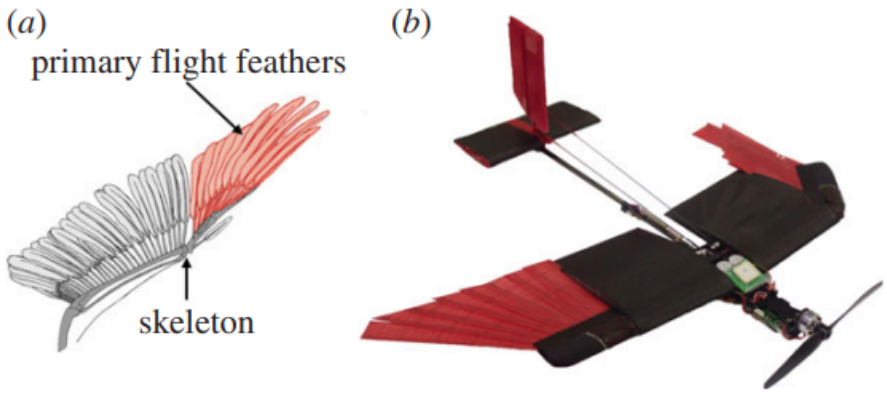

Figure 2.1: Bioinspired morphing wings, picture from [8]

performing a roll action. However, this drone is capable of rolling through asymmetrical morphing of the wings, as shown in figure 2.1, enabling the drone to roll without ailerons.

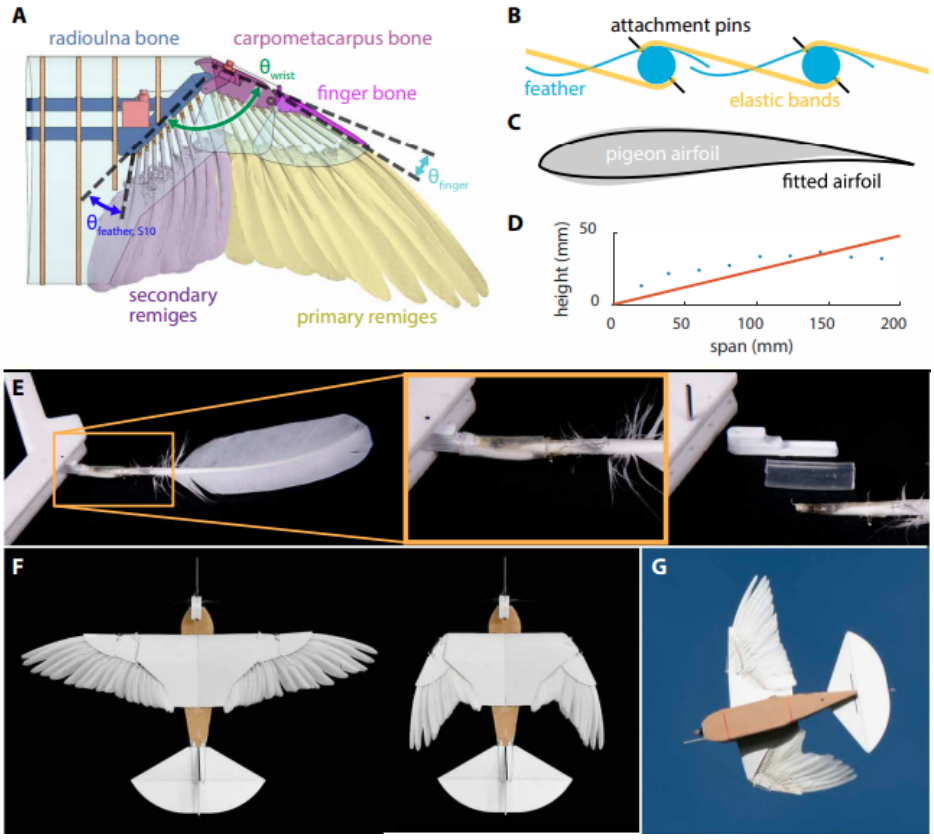

Figure 2.2: Pigeonbot, picture from [7]

[7] builds upon the prior attempts to develop a drone with feathered morphing wings. Dissimilar to previous drones that have utilized stiff feathers from materials like carbon fiber or PLA, the Pigeonbot features a

prototype with artificial feathers very similar to bird feathers. By studying the wing structure of a pigeon, the bones to which the feathers are attached have been identified, and this information was used to replicate the structure of the drone. The prototype shown in Figure 2.2 was constructed using this information.

As with the previously mentioned drone, this design also makes it difficult to install ailerons on the wings. Thus, the same method is used for this design to perform the roll action. The movement is executed by performing the actions illustrated in the G section in Figure 2.2.

2.2 Flapping Wing Micro Air Vehicles

Flapping Wing Micro Air Vehicles (FWMAVs) have reached more research interest in recent decades. Figure 2.3 showcases some examples of different FWMAVs inspired by insects. These examples are categorized into three unique types: two-winged, tandem-winged, and X-winged. FWMAVs have most commonly been researched due to their flight efficiency [28].

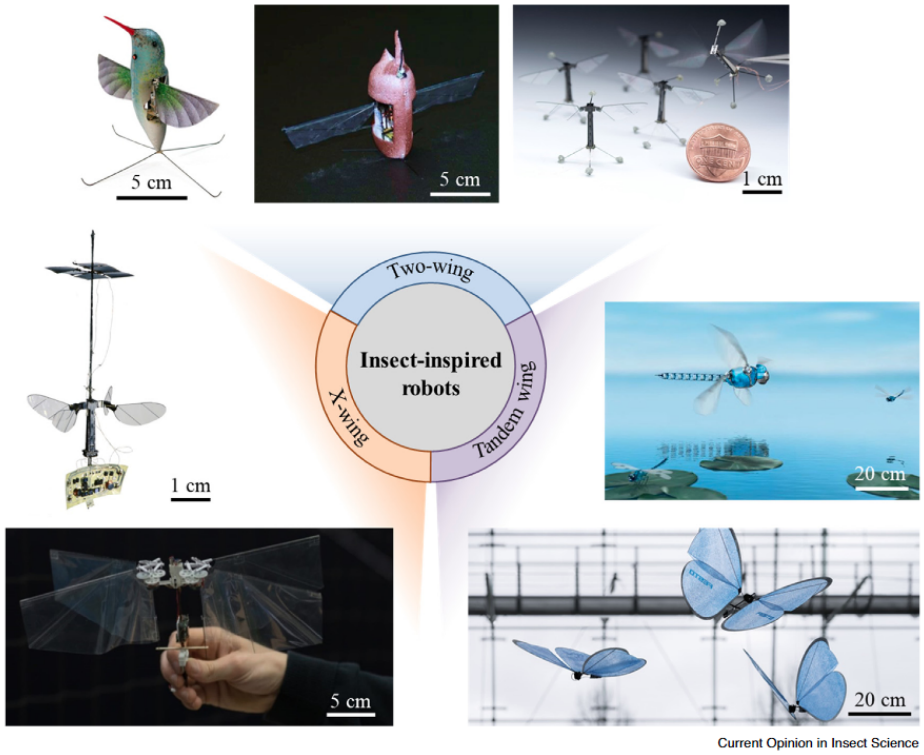

Figure 2.3: Different categories of FWMAWS, picture from [28]

Figure 2.4a features the SlowHawk2, which resembles a bird rather than an insect. The propulsion system of the SlowHawk2 consists of a crank arm that is connected to a set of gears, which in turn are connected to the motor. When the motor is activated, the wings begin flapping simultaneously. This flapping motion is the drone's only source of lift, while the tail serves as

both a rudder and an elevator to control the drone.

(a) The SlowHawk2, picture from [6] (b) The Bionicswift, picture from [22]

Figure 2.4: Various drone configurations

Figure 2.4b displays the Bionicswift, another feathered FWMAV, which was developed by Festo in 2020. The Bionicswift has a length of 44.5cm, a wingspan of 68cm, and a weight of 42 grams, and can be flown in a coordinated flock with up to five other Bionicswifts by placing radio modules in the room [22].

2.3 Drones

This section will provide an introduction to the development of drones throughout history, followed by a description of the most commonly used components in drones. Some concepts related to flight dynamics and drone development will also be explained.

2.3.1 History

The history of unmanned aircraft can be traced back to 1783, though maybe not a conventional drone, a demonstration of a hot-air balloon in France. This demonstration led to the first drone operation in 1849 when Austria loaded up 200 air balloons with explosives and sent them toward Venice [39]. In 1898, Nikola Tesla captivated the audience when he demonstrated his radio-controlled boat, a groundbreaking invention that most likely paved the road forwards for utilizing similar technology for aircraft.

Taking advantage of this new technology, there were several attempts to create radio-controlled aircraft. One of which was the Hewitt-Sperry Automatic Airplane, which was a radio-controlled airplane launched by a catapult that could fly up to 50 miles. At the same time, the "Kettering Bug" was invented by Charles Kettering, a drone that could be guided towards its target using pre-set settings. When approaching its destination, the engine was shut off, the wings would detach, and the drone would plummet towards the ground [16].

In 1935, the UK developed the first modern-day drone, which was quickly followed by the US beginning its drone program in 1936. By 1943, the US Air Force made the first First-Person View (FPV) drone, the BQ-7, which was essentially an old bomber planer stripped of everything non-essential and loaded with remote control equipment and explosives. A

pilot would take off and fly the plane nearby the target before parachuting out, allowing the plane to collide with its target.

Figure 2.5: RQ-2 pioneer, picture from [23]

In 1985, the Israeli Aircraft Industries began customizing a version of the Mastiff Remote Piloted Vehicle (RPV) for the US Navy, resulting in the delivery of the RQ-2 Pioneer in 1986, which can be seen in Figure 2.5. The RQ-2 had a length of 4.27 meters and a wingspan of 4.88 meters. The propulsion system consisted of a 29-horsepower engine giving it a total flight time of six hours and 30 minutes. This eventually led to the development of the well-known Predator drone in 1996, as seen in Figure 2.6, revolutionizing warfare by allowing pilots on the other side of the earth to control a drone capable of advanced surveillance and even engaging the enemy.

Figure 2.6: Predator, picture from [40]

Eventually, drones entered the consumer market as well. In 2010, Parrot introduced their new drone, the AR 1.0, which could be controlled via an iPhone app. The app introduced a new and exciting way of allowing

the user to view their drone's camera feed directly on their phone while operating it. Today, most commercial drones with the intention of taking photographs offer a live camera feed streamed directly to a phone, tablet, or controller screen.

Drones additionally gained additional interest during the COVID-19 pandemic, where blood tests and medical supplies have been transported by the use of drones to remote areas in underdeveloped countries. UPS even utilized drones to deliver COVID-19 vaccines in the US. The use of drones within the medical field has seen some rise in recent years.

2.3.2 What is a Drone?

An unmanned aerial vehicle (UAV), often referred to as a drone, is an aircraft capable of flying without a pilot physically onboard the aircraft. This aircraft is controlled either remotely by a pilot or by onboard software. A UAV is an essential part of an Unmanned Aerial System (UAS), which is the package required. A UAS consists of the UAV, a ground control system that has remote control over the drone.

(a) tricopter (b) Quadcopter

(c) Hexacopter (d) Octocopter

Figure 2.7: Various drone configurations

Drones are generally split into two different categories, the first of which is the multirotor. Figure 2.7 showcases four different versions of multirotors. The main difference between them is the number of motors. The names, however, are easily recognizable as they are indicated by the Latin or Greek numeral prefixes where a quadcopter has four motors, but

a hexacopter has six motors. The propulsion system of the multirotor is the vertical-facing propellers connected to the motors, and because of this, they are capable of vertical take-off and landing (VTOL).

(a) Fixed-wing drone, picture from [31]

(b) Hybrid VTOL fixed-wing, picture from [4]

Figure 2.8: Various drone configurations

The second type in the category is fixed-wing drones, as shown in Figure 2.8a. Unlike the multirotor, the fixed wing relies on its wings and forward motion to generate lift. Similar to the multirotor, this forward motion is typically achieved from one or more forward-facing propellers. As a result of this, fixed wings usually have a longer flight time than multirotors. However, conventional fixed wings are unable to hover in place, which makes multirotors more suitable for close-range photography. Figure 2.8b showcases a hybrid VTOL drone with the capabilities of both categories, utilizing horizontally faced motors to take off like a multicopter. During the flight, it can rotate the motors to face forward to utilize the efficiency of a fixed-wing drone.

2.3.3 Components

Several components are necessary and recommended for a drone to function reliably and safely. These components will be briefly explained in this section.

Flight Controller

The flight controller is an essential component of a drone that helps stabilize the drone during flight. This is done by interpreting data from available sensors on the drone, and this data is then used to adjust the speed of the motors and various control surfaces, such as the rudder and elevators. The complexity of the flight controllers varies a lot, ranging from basic flight controllers that only provide essential stabilization to flight controllers capable of autonomous flight [20].

Some key features of the flight controller are using gyroscopes and accelerometers to detect the orientation and speed of the drone to adjust the drone during flight. The ability to utilize different flight modes, such as stabilize, where the drone self-corrects to stabilize during flight, and manual, where the pilot performs all inputs, can be selected in the configuration of the flight controller. Some flight controllers also have an integrated compass and GPS, enabling the ability to navigate by GPS locations [20].

Battery

Lithium Polymer (LiPo) batteries are popular for powering drones due to their high energy density, customizable shape, and lightweight properties. They are composed of cells connected in series, so the battery's voltage depends on the number of cells. Each cell has a nominal voltage of 3.7V, so the battery in Figure 2.9, which has four cells, has a nominal voltage of 14,8V (3,7V x 4). The battery's capacity is measured in milliampere-hours (mAh) and tells the amount of energy that can be stored in the battery. LiPo batteries have a discharge rate or a C-rating, indicating the maximum amount of continuous current the battery can supply without the risk of overheating. The C-rating presents the highest continuous current that the battery can safely discharge and can be calculated by multiplying the capacity with the C-rating, so the battery in the figure with a capacity of 6500mAh and a C-rating of 80 could safely discharge up to $6,5x80 = 520A$ [30].

Figure 2.9: A traditional 4S LiPo Battery

Battery Elimination Circuit

The Battery Elimination Circuit (BEC) is a device responsible for regulating the voltage received from the battery to whichever component might need

a specific voltage, such as a flight controller. For most drones, having a device capable of regulating the voltage is crucial, as it removes the need for a separate power source. BECs have two different ways of regulating the voltage: linear BEC or switching BEC. The linear BEC converts the excess voltage into heat, thus always providing the specified voltage. This, however, wastes power and is often less effective once the voltage of the battery increases. The switching BEC regulates the voltage by rapidly switching the supply off and on again, thus resulting in less waste and heat generation [21].

ESC

Electronic Speed Controllers (ESC) are a vital component for any modern drone as it acts as the intermediary between the flight controller and the motor. The primary function of the ESC is to regulate the speed and the torque of the motors based on the input from the flight controller. So any action the pilot performs is transmitted through the flight controller to the ESC and then performed on the motor. When selecting an ESC, there are a few essential things to remember. Each ESC is designed to work with a specific voltage level, this range could, for example, be from a 2-cell LiPo battery (7,4V) to a 4-cell LiPo battery (14,8V). It also has a rating of the maximum continuous current it can handle, which makes picking an appropriate ESC for the motor crucial. Some ESCs have an integrated BEC, which can provide a regulated voltage, usually around the 5V range [17].

Inertial Measurement Unit

Section 2.3.3 mentioned that the flight controller used data from various sensors to stabilize the drone. This is done by using an inertial measurement unit (IMU) consisting of sensors such as gyroscopes and accelerometers, and sometimes magnetometers. The accelerometer measures the acceleration in the X, Y, and Z axes to stabilize the drone using the Earth's gravitational pull as a reference. The gyroscope measures the angular velocity of the drone to help maintain the stability of the drone. Moreover, the magnetometer measures the pull and direction of the Earth's magnetic field to calculate the drone's orientation. Magnetometers are often used when operating where a poor GPS signal may occur. The IMU can use data from these sensors to maintain a stable drone during flight [38].

Motors

Another crucial component for most drones is the motor. Drones have different sorts of motors, such as internal combustion engines, brushed motors, and brushless motors. Due to their efficiency, lifespan, and performance, most drones today use brushless motors, so only they will be explained here [26]. A brushless motor consists of a stationary stator and a rotor that rotates around the stator due to a generated magnetic field. Motors have a Constant Velocity (KV) rating, which indicates how many

revolutions per minute (RPM) the motor spins without a propeller when one volt is applied. This number is generally used when deciding which motor is best suited for each drone, as a motor with a higher KV will spin faster at a given volt than a lower KV motor. So, for example, a slower-flying drone with a large propeller will usually prefer a lower KV motor, whereas a high-speed drone with a smaller propeller will prefer a higher KV motor [26].

2.3.4 PixRacer

One type of flight controller typically used for more complex drones that rely on autonomous control is the Pixhawk autopilot system. The Piwhawk system is based on the open-source software PX4. One example of their autopilots is the Pixracer, designed for small drones and other RC vehicles. The pixracer has multiple sensors, such as a 3-axis accelerometer, 3-axis gyroscope, 3-axis magnetometer, and a barometric pressure sensor. The Pixracer is customizable when connecting external devices like GPS, servos, and motors [29]. These devices are easily set up with PX4 and ArduPilot software using different ground control programs, such as QGroundControl or Mission Planner.

2.3.5 Flight Dynamics

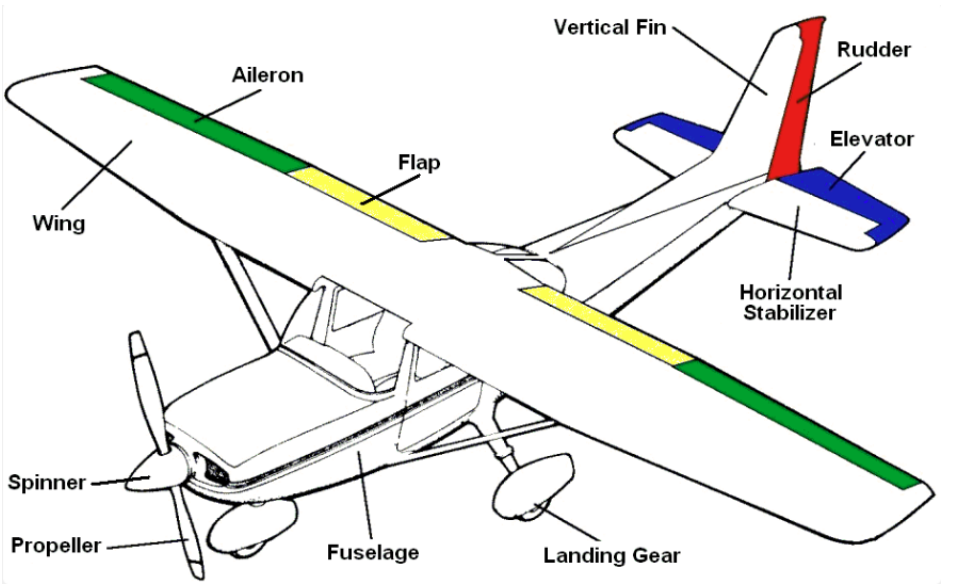

Figure 2.10: Different parts of an airplane, picture from [5]

Most fixed-wings operate identically to how most airplanes operate. The three general movements can be seen in figure 2.10 and are roll, pitch, and yaw. Roll is the rotation along the longitudinal axis and is controlled by the aileron. The ailerons are flaps attached to each wing. The flaps are connected so that when the pilot wants to steer to the right, the aileron on the right flips up, and the left aileron flips down. This motion increases lift

on the left wing while decreasing the lift on the right wing resulting in the plane rolling to the right. Pitch is the rotation along the lateral axis and is controlled by the elevator. The elevator is another flap attached to the tail of the plane. The last movement is yaw, which is a movement along the vertical axis and is controlled by the rudder. When the rudder is moved left, the tail of the plane goes in the opposite direction, which results in the plane steering to the right.

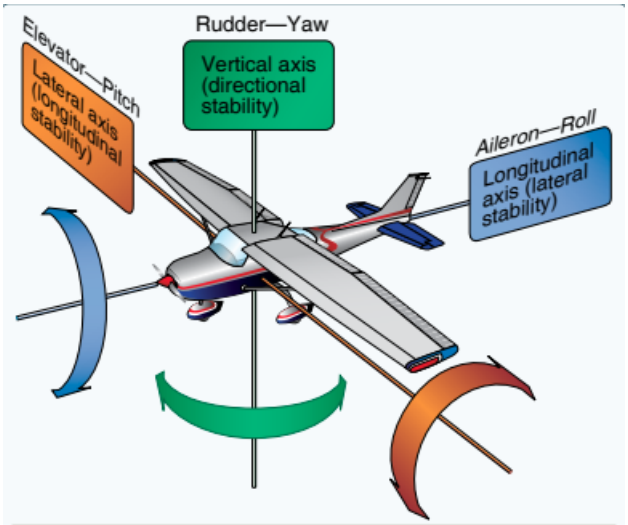

Primary Control Surface	Airplane Movement	Axes of Rotation	Type of Stability
Aileron	Roll	Longitudinal	Lateral
Elevator/ Stabilator	Pitch	Lateral	Longitudinal
Rudder	Yaw	Vertical	Directional

Figure 2.11: Flight dynamics of a fixed-wing, picture from [11]

2.3.6 Flight design

When designing the elevator and rudder of a fixed-wing drone, they must be made considering the size of the wings. However, there is no one-size-fits-all design when designing a tail, but there are some general recommendations for fixed-wing drones. Since most drones are different, there is a wide spread of information about the recommended size but listed below are some recommendations:

- **Vertical stabilizing area** 9-10% of the wing area [2] [3]
- **Horizontal stabilizing area** 18-25% of the wing area [2] [3]
- **Rudder** 25-50% of the vertical stabilizing area [2] [3]
- **Elevator** 25-50% of the horizontal stabilizing area [2] [3]

These recommendations serve as general guidance toward designing a functioning tail for a conventional fixed-wing drone. In most cases, adjusting these values to fit a specific drone might improve its control during flight.

Airfoil

Airfoils are essential to designing wings and control surfaces for fixed-wing drones, as they significantly contribute to increasing lift and reducing drag. When deciding on which airfoil to use, there are a few characteristics that are important to know.

- **Leading/trailing edge** The leading edge is the frontmost tip of the airfoil, and the trailing edge is the backmost tip
- **Camber** The camber is a description of the curvature of the airfoil's shape from the side
- **Chord** The chord is a straight line from the leading edge to the trailing edge
- **Thickness** The thickness of an airfoil is the distance between the lower and upper surfaces at the thickest point
- **Angle of attack** The angle of attack is the angle between the chord line and the direction of the airflow

2.3.7 Flight Dynamics and Characteristics

During the development of a fixed-wing drone, some essential flight dynamics must be considered to develop a stable and well-performing drone.

The Center of Gravity (CG) of a drone is a position on the drone where the drone can be held and stay balanced, meaning the weight in front of the position equals the weight behind it [37]. Typically, the CG is located slightly ahead of the center of lift in order to force the front of the drone slightly down while having an angle of attack that subsequently provides lift. These two combined factors ideally result in a stable drone capable of sustained flight. However, if the CG is positioned too far forward, in that case, the nose will be forced down, which would require additional input from the pilot or could result in an uncontrollable drone if positioned too far forward. The same applies if the CG is positioned too far back but with a rising nose instead [37].

2.3.8 Global Positioning System

Satellite Navigation is dependent on a network of satellites that orbits around the Earth. The most well-known system used is the Global Positioning System (GPS), which was developed and maintained by the United States. This system consists of 31 satellites that broadcast signals to

receivers, enabling them to determine their location when connected to at least four satellites [12].

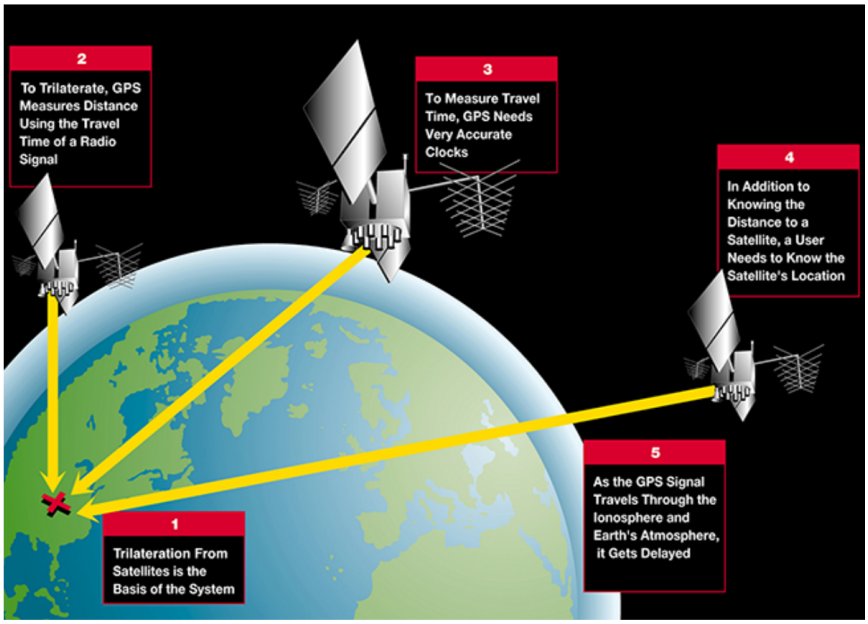

Figure 2.12: Illustration of GPS, picture from [12]

The satellites utilize atomic clocks when transmitting time and their current location. Hence, the receiver can calculate the signal's travel time from the satellite to the receiver to determine the distance between the user and the satellite. With access to three satellites, it is possible to calculate a three-dimensional position using the time data. An illustration of this can be seen in Figure 2.12. However, with access to a fourth satellite, knowledge of the time is no longer necessary to determine the user's latitude, longitude, altitude, and time [12].

2.4 3D-printing

Three-Dimensional printing (3D printing) is an additive manufacturing process that creates a 3D object from a 3D model. This process enables a user to design complex objects using different Computer-Aided Design (CAD) programs and then have these objects printed in different materials. 3D printing is a preferred manufacturing method in many fields involving things such as rapid prototyping, creating custom parts, and manufacturing consumer goods. 3D printing usually follows the order in the list below:

- **Design** Create or find a 3D model online and convert it into a suitable file format, such as Standard Tessellation Language (STL)
- **Slicing** The STL file is sliced in a program typically designed for each brand of 3D printer, where the different layers of the print can be inspected and modified if desired.

- **Printing** The sliced file is provided to the printer with the desired material loaded. These materials are printed layer by layer until the print is finished. Different materials will be covered in Section 2.4.
- **Post-processing** When the print is finished, additional work is often required, such as removing support, removing the platform beneath the print, or even polishing the print.

3D Printing Materials

Polylactic Acid (PLA) is a commonly used material for 3D printing and is a biodegradable thermoplastic polymer made from various renewable resources like corn starch. It has many properties making it an ideal material for 3D printing, such as its environmentally friendly biodegradability. It also has a relatively low melting temperature compared to other 3D printing materials, melting at 180-220°C varying between manufacturers. In addition, PLA is known for how easy it is to print, being a very accessible printing material for beginners. However, it is less durable and more brittle than other printing materials such as Acrylonitrile Butadiene Styrene (ABS) and Polyethylene Terephthalate Glycol (PETG), making PLA less suited for high impact and long-term durability applications [36].

Another material used for 3D printing is Lightweight PLA, also known as foaming or expanding PLA. Lightweight PLA is a modified type of PLA that has been incorporated with a foaming agent to create a lighter and less dense final product. This material is often used instead of regular PLA for applications where weight is essential, such as drones and other remote-controlled vehicles. In addition to creating a lighter finished product due to the foaming, this material also reduces the amount required, thus reducing the cost. There are, however, some trade-offs. The structural strength of lightweight PLA is generally lower than regular PLA. Additionally, printing it is considered more challenging than regular PLA in order to achieve the same results [13].

Chapter 3

Method

This chapter will first present some of the ethical considerations that must be considered when developing and operating drones. Then, an overview of the methods explored and their progression is documented through several revisions.

3.1 Ethical Considerations

The ethical considerations to consider surrounding drones are crucial to take into consideration when beginning to develop one. The predominant concern about drone operations and development is related to safety and privacy regulations. Furthermore, autonomous drones and potential weaponization have become a concern with the introduction of AI in recent years.

In Norway, the transition to the new EU regulation began on the 1st of January 2021. These regulations are published by the Norwegian Civil Aviation Authority, or Luftfartstilsynet[1], which provides all necessary precautions and restrictions for drones of various weights. In addition to the operational regulations from Luftfartstilsynet, the regulations related to sensors also needs to be considered. Regulations on sensory systems such as cameras, IR sensors, and radars can be obtained from the Norwegian National Security Authority[2] (NSM).

The advent of autonomous drones has been a topic of discussion related to autonomous weapons. The future of Life[3] (FLI) was founded in 2014 and has taken a point of steering this conversation. The FLI was founded to guide humanity in the right direction when world-changing technology is discovered. They have created multiple pledges concerning lethal autonomous weapons. One of these [4] is signed by several noteworthy individuals such as Demis Hassabis, Shane Legg, and Mustafa Suleyman of Deepmind, and SpaceX's Elon Musk, among others.

[1] https://luftfartstilsynet.no/en/
[2] https://nsm.no/home/
[3] https://futureoflife.org/
[4] https://futureoflife.org/open-letter/lethal-autonomous-weapons-pledge/

While this project does not fall into the category of autonomous weaponry, it is essential to recognize the potential misuse of drone technology for malicious purposes. Throughout the last few years, drones have been used more and more for activities like drug smuggling and the deployment of explosives. Therefore, recognizing it as a reality is essential even though it is not the project's purpose.

3.2 Overview

During the literature review, plenty of information on morphing wings for airplanes was discovered, but the research on morphing wings for drones had limited results. Because of this, the literature review was divided into two parts: general morphing wings and morphing wings specifically for drones. In Section 2.1, several drones with morphing capabilities were discovered, and a few of these will act as inspiration for the first designs. The findings from the background chapter revealed that increasing the area of the wings resulted in more lift produced but also made the drone more susceptible to strong wings. On the other hand, reducing the wing's area enhanced the drone's aerodynamics by reducing drag, allowing it to reach higher speeds. This project will develop a drone that can utilize the best of both scenarios by designing and developing a drone with wings capable of morphing.

In order to narrow down the scope of this project, it was necessary to decide the extent of morphing capabilities to explore. The first method to be explored in this chapter will be a mechanism capable of performing the most basic form of morphing wings. This method involves reducing the wing's area by folding the outer edge into the wing, effectively reducing the area of the wing. This method will then be tested to determine its viability before being implemented on a drone. If it proves successful, it will be installed in a drone and tested by conducting various tests in a lab setting and, eventually, test flights. Throughout the experiments, the Technology Readiness Level (TRL) displayed in Figure 3.1 will be guiding the development toward a desirable solution. The first two steps of the TRL were already covered in chapters one and two, with details about related works and general information about drones and morphing wing technology.

Throughout the experiments, the technology readiness level (TRL) displayed in 3.1 will be used to guide us toward a desirable solution. The first two steps of the TRL were covered in chapters one and two and consisted of research into similar projects and general information about drones and bio-inspired drones, such as morphing wings and feathered drones.

To facilitate the testing, Autodesk Inventor will be used to create sketches and assemblies. This will allow us to evaluate the functionality of components and even entire methods before moving forward. Once a method has proven viable in an Inventor assembly, it will be created using suitable materials, such as foamboard or 3D-printed PLA, to bring

Figure 3.1: TRL, picture from [35]

the design to life. It will also be experimented with alternative materials to determine which is best suited for each task. Once a viable method capable of adjusting the shape of the wings has been developed, stage three in the TRL has been reached, having an experimental proof of concept.

When a suitable method of morphing the wings has been discovered, it will be installed on a drone to continue testing to reveal any possible errors. Level four in the TRL will primarily consist of lab testing, where the morphing mechanism will be evaluated in a lab environment. Once verified, step five in the TRL will begin, which will involve testing the drone outdoors and conducting test flights to continue evaluating the performance of the morphing mechanism.

3.2.1 Main Idea

A scaled-up drone version will be created to verify that the current morphing mechanism being tested is viable. However, to get ideas into reality, a simple drone body was designed in Autodesk Inventor. This drone body can be seen in Figure 3.2a. This design consists of a simple drone body with an opening at the top to allow for easy access to components and the battery while having an attachable wing that will cover the opening during flight.

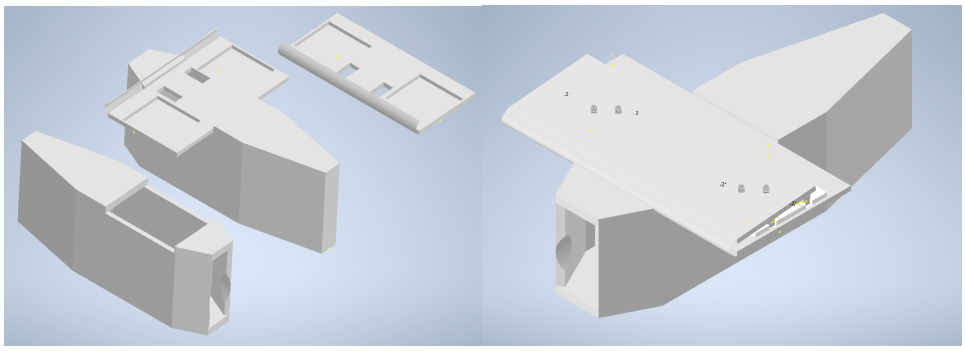

(a) Inventor design of body (b) Inventor sketch with wings

Figure 3.2: Drone sketches and prototypes

Figure 3.2b displays the Inventor sketch of the drone with the attached wings. The wings are designed to fit atop the drone and will be attached through the use of rubber bands. The wings are designed in such a way that they can be folded onto themselves to incorporate a more aerodynamic profile rather than just being a flat piece of foamboard.

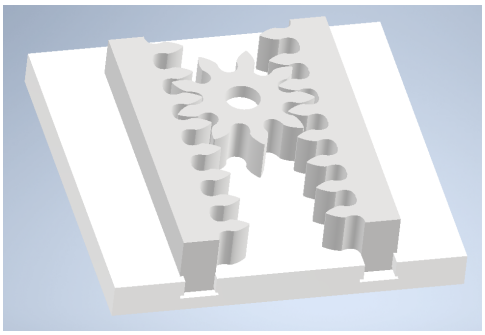

Figure 3.3: Morphing mechanism

The sliding bracket used for the morphing mechanism can be seen in Figure 3.4. As can be seen, the side has protruding pins that allow the cogwheel to move when the opposite sliding rack is moved. Additionally, the bottom (top in the image) is shaped to be installed in the platform in such a way that it can move left and right while not risking falling out.

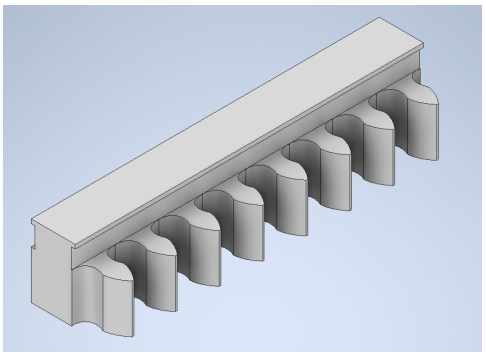

Figure 3.4: sliding bracket in the morphing mechanism

Figure 3.5a displays the initial sketch of the body design. The primary objective of this draft was to produce a preliminary sketch that can be utilized as a reference, given that the initial body is intended to be constructed using foamboard. The design was developed to ensure that each distinct component can be effortlessly created using foamboard. The first draft of the body, made entirely out of foamboard can be seen in Figure Figure 3.5b.

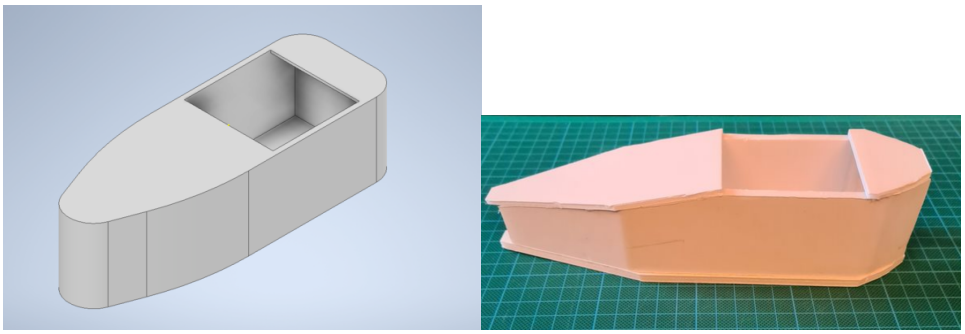

(a) Body 1 sketch (b) body 1 prototype

Figure 3.5: Drone body first draft

This design will consist of a rudimentary version of a morphing wing that is able to alter its wing area. This idea is inspired by the design of the pigeonbot [7], which was mentioned in Section 2.1. The initial design will mimic the design of the Pigeonbot but on a simpler scale and without the use of feathers. The wing will be split into two distinct parts: the middle part, which will be attached to the body and contain a predetermined position for the required servos. Secondly, the outer limbs, which will function as the wings are responsible for adjusting the wing area by either being fully extended or withdrawn into the middle part.

Furthermore, to successfully control the movement of the outer limb, a mechanism responsible for adjusting it is required. This mechanism must be capable of retracting the outer limb into the folded layer of foamboard, also known as the middle piece. Figure 3.3 showcases the mechanism that will be utilized for this method. A sliding bracket, displayed in Figure 3.4, is affixed to a 50x50mm platform to keep it in place. When the sliding

bracket is inserted into the platform with the cogwheel secured in the middle, it is only able to move left and right, as depicted in Figure 3.6.

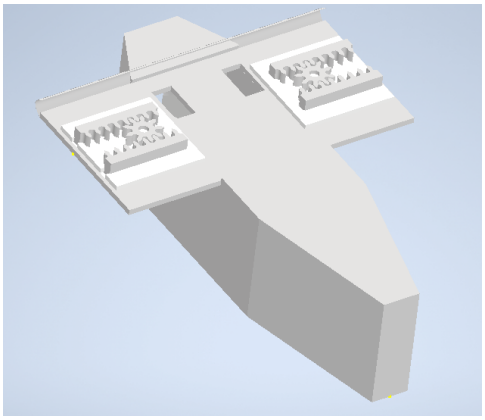

Figure 3.6: Inventor sketch with morphing mechanism

The first physical prototype of the body can be seen in Figure 3.7. This body was constructed by cutting the bottom and the sides using the dimensions from the Inventor sketch and then joining them together using glue. Additionally, two pieces were attached to the top of the body to reinforce the walls. Dissimilar to the sketch, the rear end of the body was made in a descending manner, further reducing the overall weight. An opening was created on the top of the body to provide easy access to the interior of the drone for easy access to components and battery changes. The body was created using 5 mm foamboard.

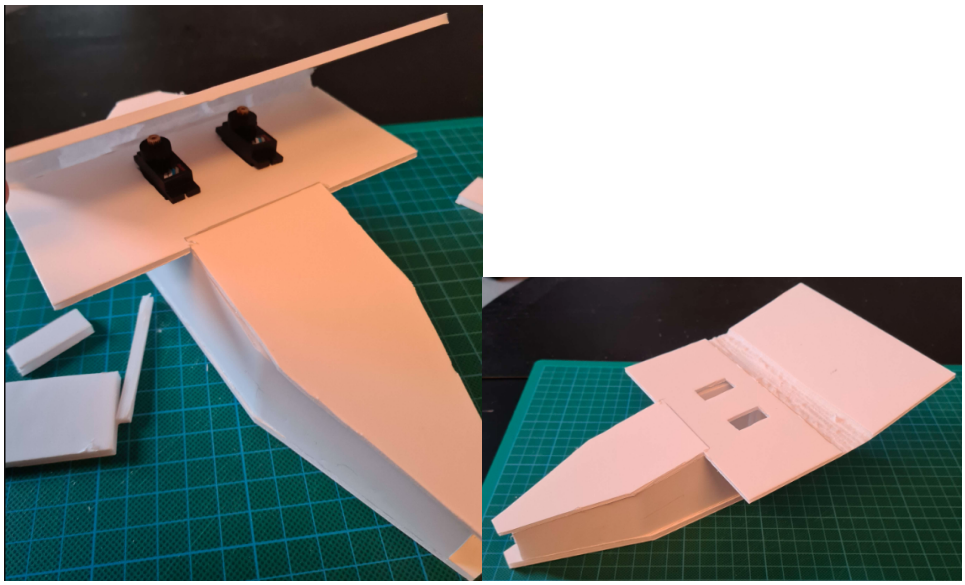

(a) Drone prototype without servos (b) Drone prototype with servos

Figure 3.7: Drone prototypes

The wing, made separately from the body, can be seen lying atop the

drone in Figure 3.8a. As the morphing mechanism required two separate servos, two holes were made in the wing's interior where these will be installed. These servos will be installed from below to minimize the space required in the fold of the wing. Considering that structural strength is not a crucial element for the wings, they were made out of 3 mm foamboard.

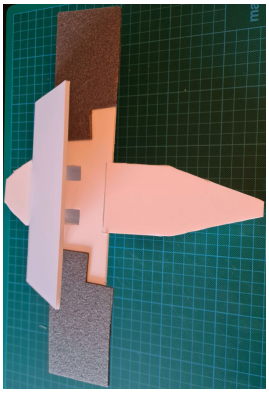

(a) Example of wing extensions

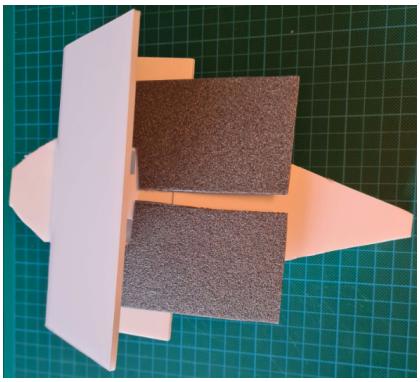

(b) Example of wing extension

Figure 3.8: Example of wing extension side

Picture 3.8a illustrates the concept of this morphing mechanism, with the black Depron pieces acting as the outer limbs attached in a single point to enable folding. Through the use of the previously mentioned morphing mechanism, these outer limbs can be adjusted during flight to reduce the wing area of the drone. The Depron pieces in the figures are attached in a single point with a screw, enabling them to fold into the wing.

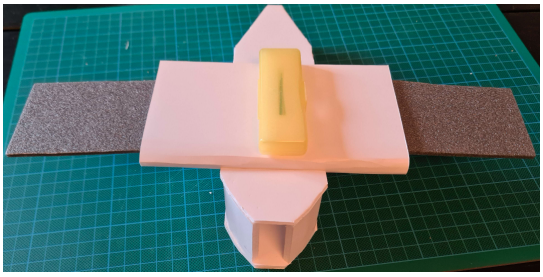

(a) Example of wing extensions

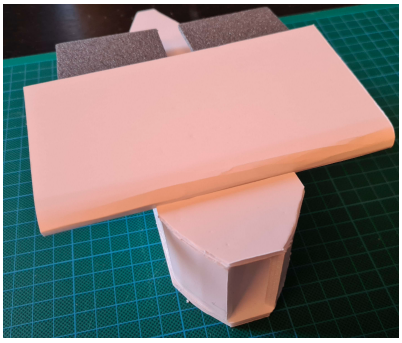

(b) Example of wing extension

Figure 3.9: Example of wing extension front

Figures in 3.9 show how it would look when the wing overlaps the wing extension. As the wing extensions are currently made of Depron, the exploration of finding a suitable design and the appropriate material for the wing extensions can begin once the morphing mechanism has been tested.

The designed morphing mechanism will be installed in the middle of

the body, with each wing having its respective mechanism. Furthermore, each morphing mechanism will have its respective servo to enable unsynchronised control to be able to roll. When installed, it can extend the wings by pulling the frontmost sliding bracket toward the center of the body, thus moving the opposite sliding bracket away from the body. By attaching the wing's extended limb to the backmost sliding bracket, this movement will, in turn, withdraw the outer limb by a method that is yet to be designed. This method of morphing was pursued due to the nature of the design, which utilizes the sliding bracket and a cogwheel. A spring could be installed to support the servos in keeping the wing extension extended by keeping constant pressure on it. This support could be helpful if the servos are unable to keep the wing extensions extended during the flight due to the airflow.

As the construction phase was being navigated, there was still the task of designing an elevator and rudder for the drone's pitch and yaw control. The tail will be created by attaching a carbon fiber rod to the body, and on the end of this rod, an ordinary rudder and elevator will be made out of foamboard to keep the weight to a minimum.

After 3D printing all the necessary components and subsequent tests of the morphing mechanism, a series of challenges occurred that made it difficult to implement. One of the most significant issues was accommodating all the components within the folded wing, severely limiting the size constraints for each component. Additionally, to make the sliding brackets slide as smoothly as possible, a highly precise 3D print was required, which proved to be an issue. Due to these challenges, it was decided to explore alternative methods for achieving morphing wings on the drone.

Fortunately, the testing phase did provide valuable insight into potential issues and corresponding solutions that can be utilized in the alternative approach. The following section will explore this alternative method, focusing on finding a suitable method of morphing the wings, with a focus on testing and refining the design, as well as the drone's wing and control surfaces.

3.3 Prototype Two - Other Sliding Method

The second method being explored involved removing the cogwheel and the sliding brackets, opting instead to use the servos directly to adjust the wings. This method will employ the same body that was utilized for the previous prototype, as the size and shape will also fit this concept. The following chapter will describe the main idea behind this prototype and introduce the initial components used for it. Further versions of this prototype will then be presented, where the most significant changes in each revision will be described. At the end of each revision, a table listing all components used in that revision is included.

3.3.1 Main Idea

The main components of this method are displayed in Figure 3.10 with the sliding base, which can be seen in Figure 3.10b. Attached to the sliding base is the green piece, now referred to as the sliding rack. This piece can be seen in Figure 3.10b. Figures 3.10c and 3.10d showcase how the sliding rack can be moved using the servos installed in the middle. To provide lift to the drone, artificial feathers will be affixed to the sliding base and the sliding rack.

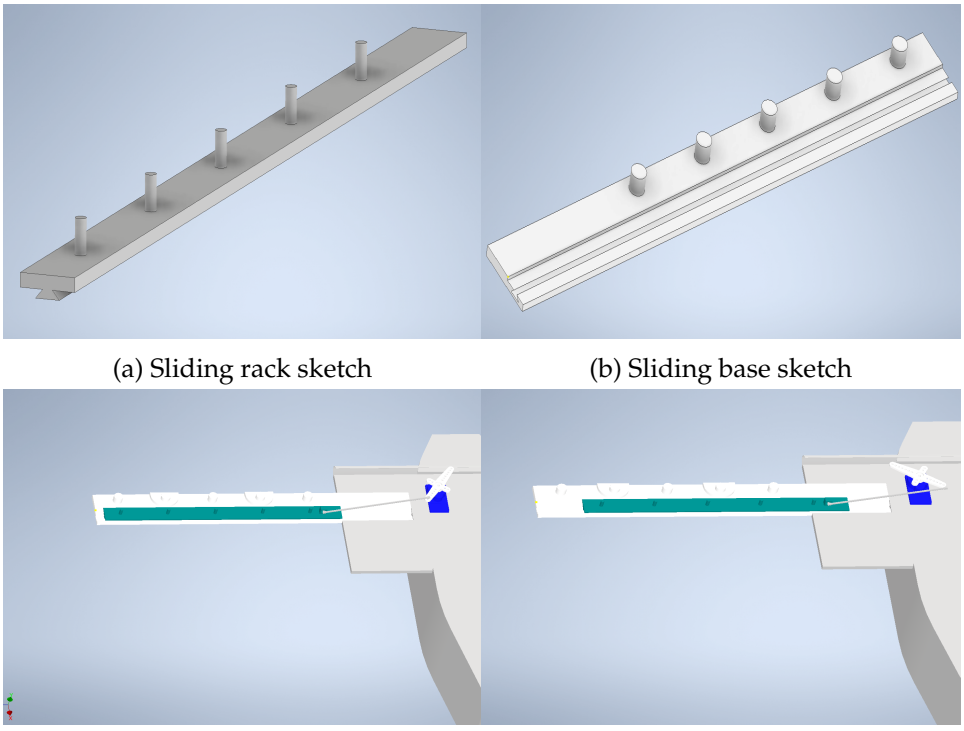

(a) Sliding rack sketch

(b) Sliding base sketch

(c) Inventor assembly of wing in extended position

(d) Inventor assembly of wing in withdrawn position

Figure 3.10: Sketches of components

3.3.2 Initial Prototype

As was mentioned in Section 3.3.1, this morphing mechanism relies on using the sliding base and rack in order to adjust the wings. In order to install these components on the drone, a wing platform was designed. This wing platform can be seen in 3.11a and will be installed to sit on top of the body, to which the sliding base can be attached. The earliest drafts of the sliding base and sliding rack can be seen in Figure 3.11, in addition to a first draft of the feather. Once a suitable design for the feathers has been decided, it will be covered in an airtight material to fill the gaps. As depicted in Figure 3.11b, the base of the feather is slightly elevated to allow the feathers to fold on top of each other without colliding.

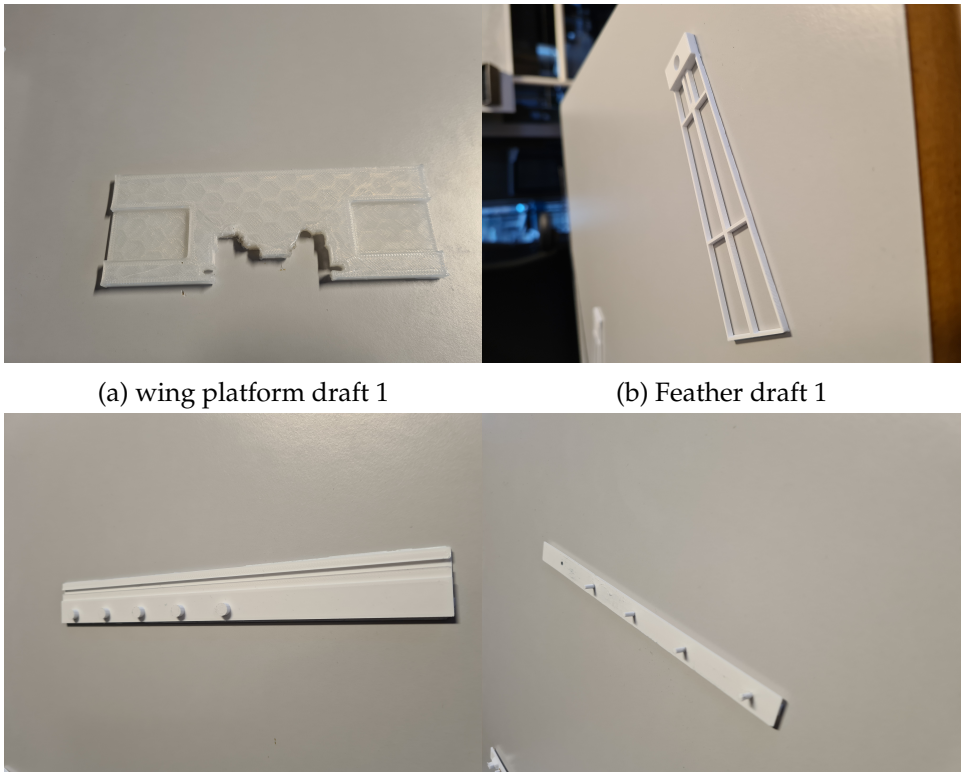

(a) wing platform draft 1 (b) Feather draft 1

(c) Sliding base draft 1 (d) Sliding rack draft 1

Figure 3.11: First drafts

Figure 3.12 shows how all the pieces will be installed in the middle piece, where the sliding base will be attached using glue. Figure 3.12a displays the feathers' layout once installed on the sliding base (without the foamboard piece), and Figure 3.12b illustrates how the servos are attached to the middle piece and connected to the sliding rack through the use of piano wire and a 3D-printed attachment. However, difficulties with the servos not consistently withdrawing the sliding rack were encountered during testing. Therefore, it was decided not to install this mechanism on the drone before these issues were addressed, which will be described in the next section.

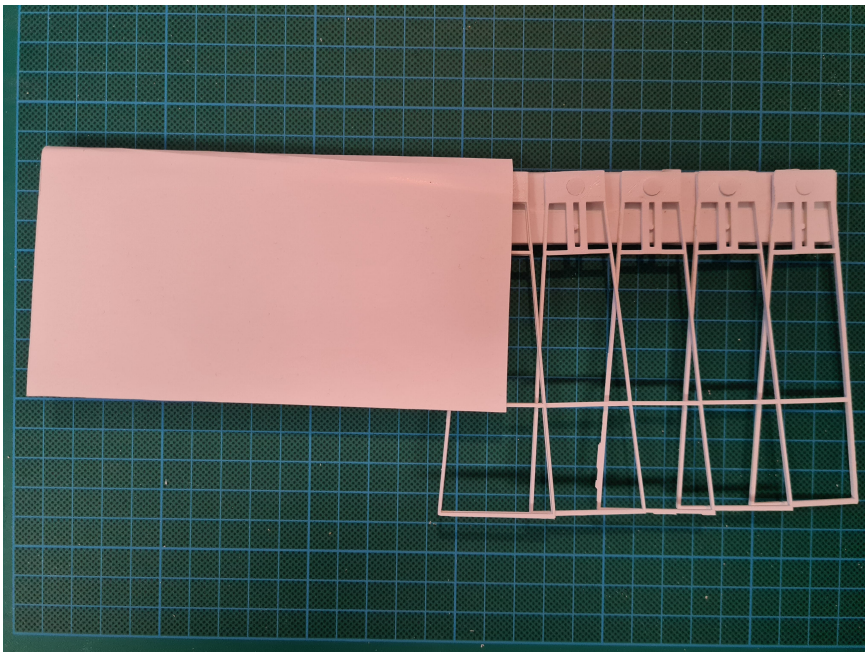

(a) Feathers installed on sliding base

(b) Servos and sliding base installed on wing platform

Figure 3.12: Early installation of morphing mechanism

Table 3.1: Comonents used for the initial prototype

Component	Currently used component
Morphing mechanism Servo	Dualsky DS395 Digital Micro Servo 1.5kg/0.10s
Battery	3s 2200mAh - 20C - Gens Ace Soaring Mini XT60
Radio	Taranis X9D

3.3.3 Revision One

The first significant change for the first revision entailed removing the elevated base of the feathers with a modified sliding base. A visual representation of this can be seen in Figure 3.13a, which showcases the sketch and the 3D print of the adjusted sliding base. As can be seen here, alternating pins feature an elevated base to regulate the height of the feathers. Additionally, since an elevated base was no longer required for the feathers, it was decided to redesign and extend their length to generate additional lift. A sketch of the redesigned feather and a 3D print of it can be seen in Figure 3.13b. This Figure shows that the new feather weighs 3 grams, resulting in a total weight of 30 grams for the ten plans that will be used.

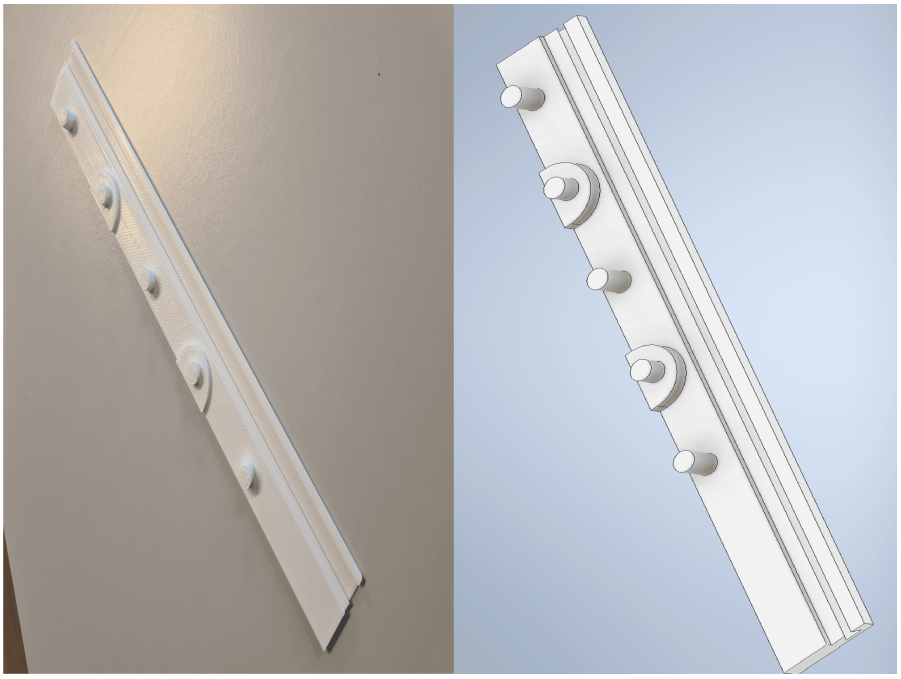

(a) Sliding base sketch and prototype revision one

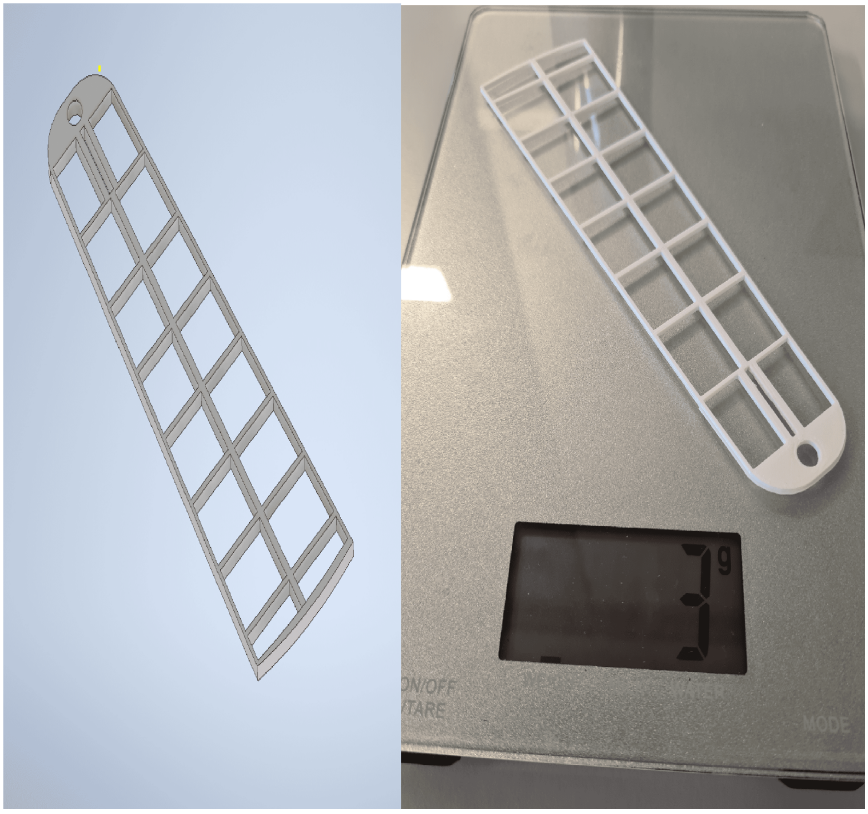

(b) Feather sketch and prototype revision one

Figure 3.13: Sketches and prototypes for revision one

The motor plays an essential role in any fixed-wing drone as it serves as

the sole means of propulsion. A motor holder was specifically designed to ensure that the motor remains securely in place during flight. As most of the drone body was made of foamboard, a practical solution was needed to attach the motor holder to the body while keeping the motor in place. This motor holder, including a sketch and a prototype, is depicted in Figure 3.14.

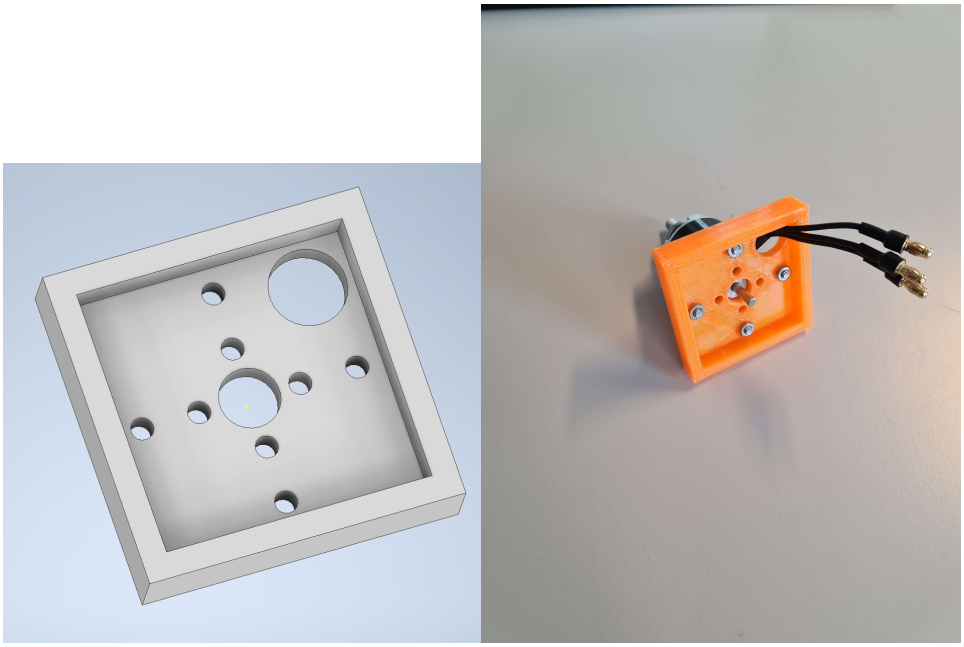

(a) Inventor sketch of motor holder (b) Motor holder prototype

Figure 3.14: Motor holder sketch and prototype

In order to securely attach the morphing mechanism to the drone body, it was decided to 3D print a support mechanism instead of attaching wooden pieces to the sides of the drone body, which is a common practice in fixed wings. This component can be seen in Figure 3.15, highlighted in blue. The primary function of this addition is to provide support for a carbon fiber rod that will go through the body and protrude from both sides. Using this rod, the morphing mechanism will be attached to the body using rubber bands or a similar method. If the rod were to be inserted through the body without the support, the foamboard would likely break from the pressure exerted by the rubber bands.

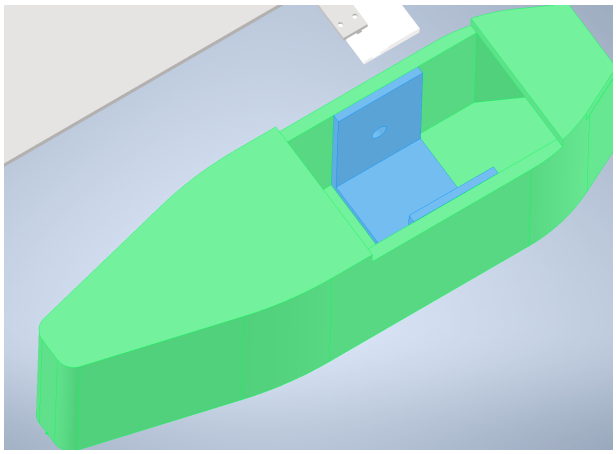

Figure 3.15: Support for attaching the wings

Having implemented these revisions, everything was assembled in order to evaluate the servos' ability to withdraw the feathers. During testing, it was observed that the pins on the sliding rack did not display the anticipated sturdiness, as they started to loosen after a few tests. Moreover, during 3D printing of the sliding rack, it was necessary to have either the bottom (the part that slides into the sliding base) or the top (the side featuring the pins) resting on the printing bed, requiring the addition of support to the print. When the bottom of it was positioned on the printing bed, it proved challenging to remove all of the support, leading to unnecessary friction between the sliding base and the sliding rack. However, if it was printed with the top facing the printing bed, the pins intended for attaching the feathers often came loose during the removal of the support. In light of these issues, the need to redesign the sliding rack was recognized, which will be covered in the next chapter.

Table 3.2: Components used for revision one

Component	Currently used component
Morphing mechanism Servo	Dualsky DS395 Digital Micro Servo 1.5kg/0.10s
Motor	Dualsky ECO 2312C V2 960KV 58gram
Battery	3s 2200mAh - 20C - Gens Ace Soaring Mini XT60
Receiver	FrSky S6R 6 channel Receiver with 3-axis Stabilization
ESC	Hobbywing SkyWalker 30A ESC
Radio	Taranis X9D

3.3.4 Revision Two

After testing different revisions of the morphing mechanism, it was noticed that the bottom piece of the drone body started deteriorating from

repeatedly attaching pieces with glue. Because of this issue, the design of the next version of the body was started, which can be seen in Figure 3.16a. The second draft kept many of the same principles as the first draft. Additionally, this draft is made with a 3D-printed bottom piece to provide better precision when attaching the walls and is showcased in Figure 3.16b. However, replacing the largest part of the body with a 3D-printed counterpart will result in an increase in weight. This increase can be seen in Figures 3.16c and 3.16d, which display an increase from 17 grams to 36 grams, doubling the body's weight.

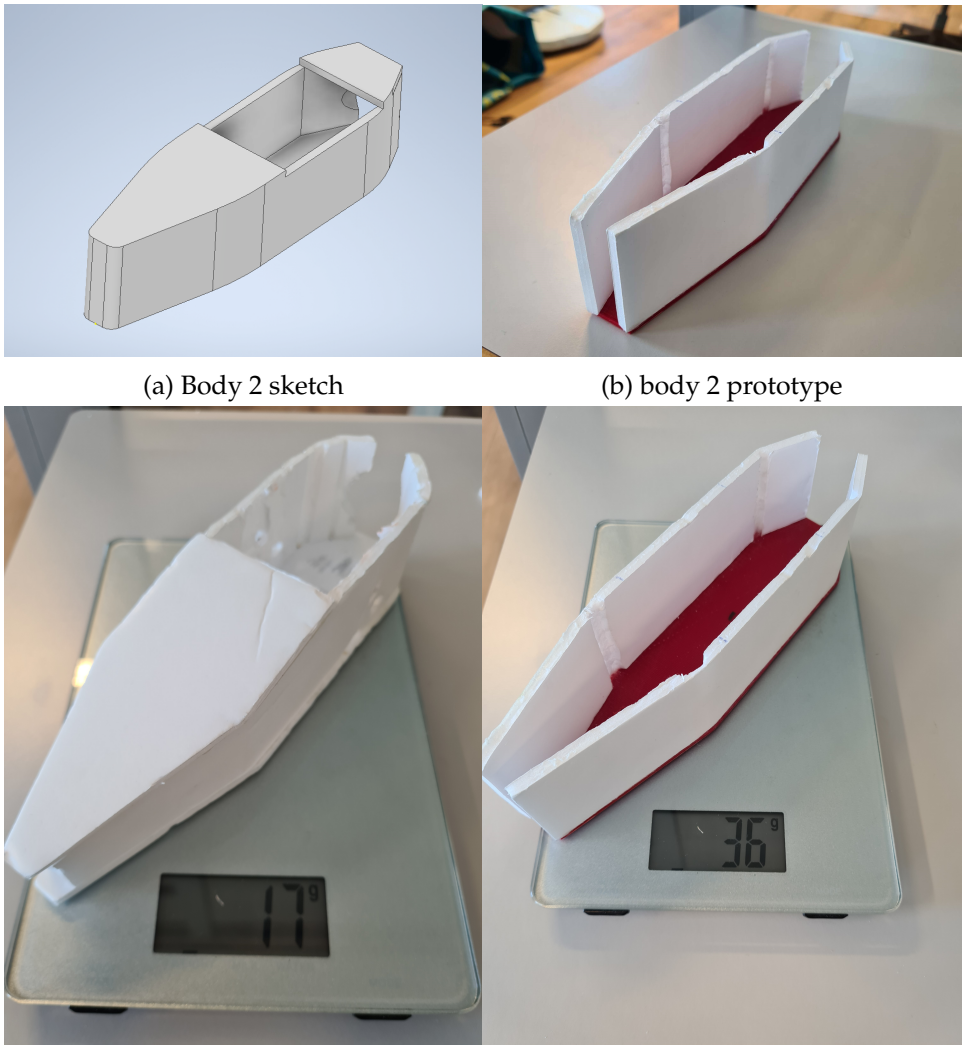

(a) Body 2 sketch

(b) body 2 prototype

(c) Body 1 weight

(d) body 2 weight

Figure 3.16: Drone body revision two

As mentioned in chapter 3.3.3, difficulties with the pins on the sliding rack breaking after repeated use was experienced. In order to circumvent this issue, the sliding rack will now be printed with the part that slides in the sliding base facing away from the printing bed. However, because of this, a new method of attaching the feathers to the sliding rack had to be

investigated.

Figure 3.17 displays a pair of sketches showcasing the sliding rack's new sketches. From this Figure, it can be seen that the original pins have been removed, and in their place, screws will be introduced that will function in the same role. Figure 3.17a highlights an indent in the sliding rack, specifically designed to accommodate the screw head. Furthermore, to enable a smoother folding, every alternate feather now has an elevated base similar to the sliding base.

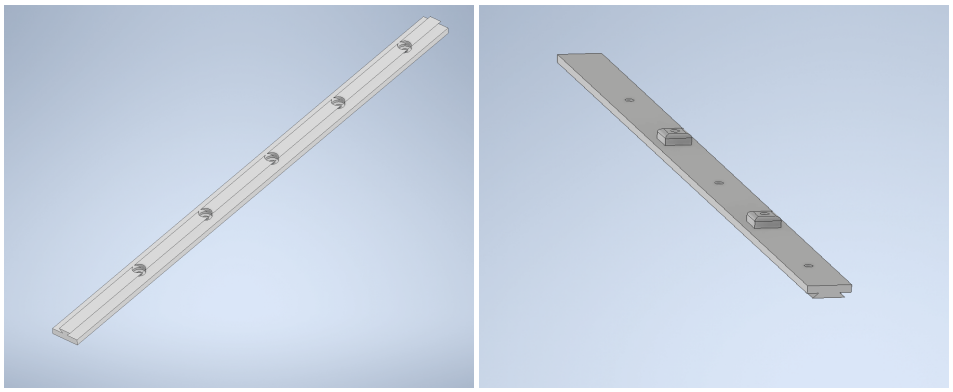

(a) Sliding rack sketch (b) body 2 prototype

Figure 3.17: Sliding rack sketch and prototype revision two

The completed prints of the redesigned sliding racks are depicted in Figure 3.18. These figures also feature the servo attachment attached to the end of the sliding rack. M2 screws have been employed for this design, with 8mm screws being used for the non-elevated holes and 14mm screws for the elevated holes. Figure 3.18b demonstrates the seamless integration of the screw heads into the sliding rack, ensuring there is no protruding to interfere with the movements within the sliding base. However, Figure 3.18c reveals the uneven surface resulting from the support structures. Because of this, the outer edges of the feathers were filed down using sandpaper to achieve a smoother finish.

(a) Sliding rack from below

(b) Sliding rack from the side

(c) sliding rack from above

Figure 3.18: Different points of view of the sliding rack

With the redesigned feather, it was deemed appropriate to start attaching the air-tight material to evaluate how much of an impact this had on their flexibility. The material used for this attempt was originally intended for mending windsurfing sails. A complete feather featuring the cover can be seen in Figure 3.19, which also displays the current weight of 5 grams. This is an increase of 2 grams from the original weight of 3 grams. The incorporation of the material significantly increased the feather's strength, as the material is glued onto all of the internal support of the feather, resulting in a stiffer feather. In addition to the previously mentioned changes to the sliding rack, the piece on the sliding rack that is inserted into the sliding base was reduced in size in an attempt to reduce friction between them. As a start, the width was reduced by 1 mm to determine how much of a difference it would make when assembled.

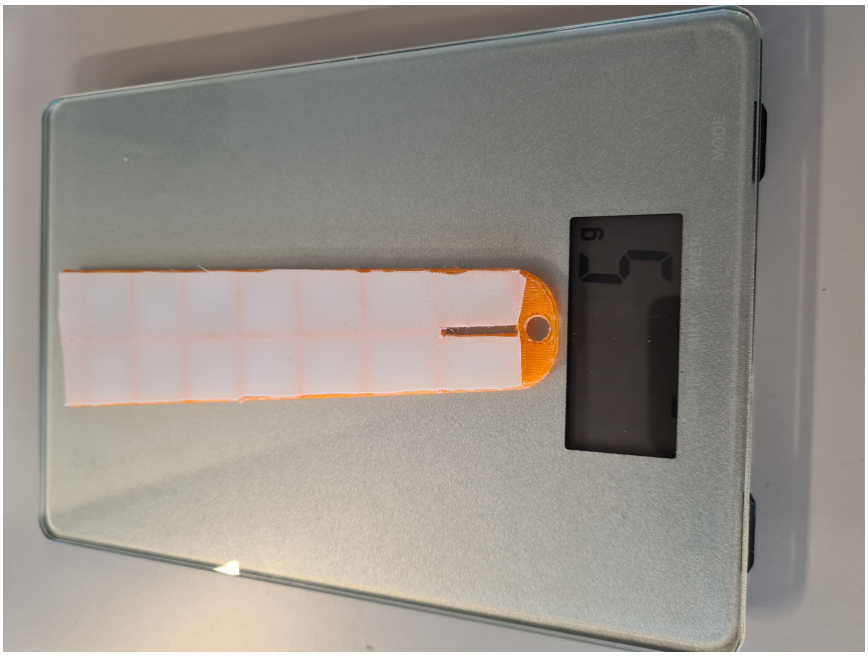

Figure 3.19: Covered feather

As the previous foamboard wing cover for the mechanism was removed for this prototype, a need for an alternative solution that could shield the front of the sliding base from airflow was recognized. This new wing cover could also give the wings a more aerodynamical shape. A wing cover that conveniently fastens to the same pins as the feathers, was designed to address this issue. A sketch of this wing cover is presented in Figure 3.20a, while Figure 3.20b showcases how this looks when installed on the wing. As can be seen, this cover functions as a shield against the air, as well as a means of fastening the feathers to the sliding base.

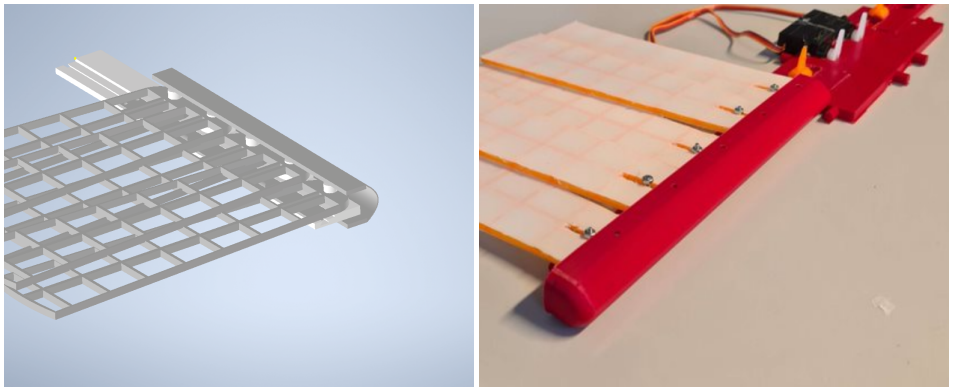

(a) Wing cover assembly (b) Wing cover installation

Figure 3.20: Wing cover

With all of the modifications previously mentioned in this section implemented, the assembly of the drone began in order to evaluate the servos' ability to withdraw the feathers. Figure 3.21a presents

a representation of the assembled morphing mechanism of the drone, including how the rubber bands will secure all components in place during flight. Figure 3.21b displays a demonstration where the left side is fully withdrawn with the feathers resting on top of each other and partly resting on the drone body, showing how the drone would look during a roll motion to the left. Using this assembly of the morphing mechanism, the servos were connected to the servo, and all necessary configurations were done to test the morphing mechanism.

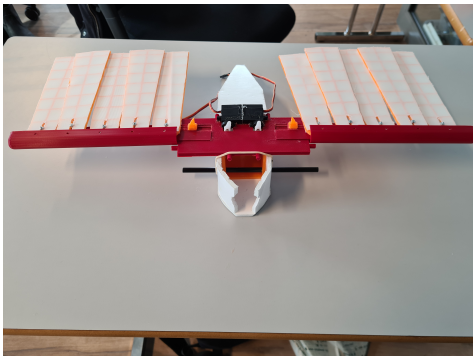

(a) Revision two assembled

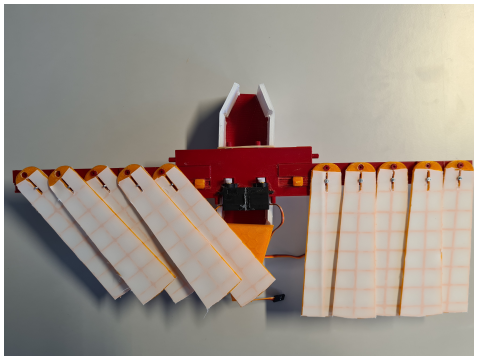

(b) Revision two assembled

Figure 3.21: Assembled version of revision two

Nevertheless, the testing revealed that even though the servos could withdraw the feathers appropriately, they used, on average, two seconds to withdraw them from a fully extended position. Moreover, difficulties in adjusting the range of the servos using the receiver were experienced. In an attempt to resolve these issues, it was decided to upgrade the servos and incorporate a PixRacer instead of a traditional receiver. The integration of these new components will be covered in the following section.

Table 3.3: Components used for revision two

Component	**Currently used component**
Morphing mechanism Servo	Dualsky DS395 Digital Micro Servo 1.5kg/0.10s
Motor	Dualsky ECO 2312C V2 960KV 58gram
Battery	3s 2200mAh - 20C - Gens Ace Soaring Mini XT60
Receiver	FrSky S6R 6 channel Receiver with 3-axis Stabilization
ESC	Hobbywing SkyWalker 30A ESC
Radio	Taranis X9D

3.3.5 Revision Three

The previous chapter mentioned the decision to upgrade specific components to increase the morphing mechanism's speed. Additionally, as a testable product is approaching, a PixRacer was integrated into the drone to be able to utilize all functions provided by ArduPilot. Since the PixRacer has several components required to function correctly, including GPS, a safety switch, and a power module, several components have to be redesigned to accommodate the increasing number of components from the PixRacer.

With the increasing number of components required for the morphing mechanisms, the size of the drone body became a crucial factor. Therefore, a third body iteration was designed, portrayed in Figure 3.22a. Notably, this design features a customized back compartment with a predetermined position for the battery. Additionally, small indents have been made to ensure predetermined positions for the pixracer and the ESC. A small circular opening can also be observed at the back of the body where the tail will be attached. A carbon fiber rod with a diameter of 7mm will be inserted into the back of the drone, and at the end of this carbon fiber rod, a rudder and elevator will be installed. For a visual representation of this design, refer to Figure 3.22b, which displays the body printed in PLA. While the final version of this design will be printed in lightweight PLA, the early prototypes are being printed in regular PLA as it is more accessible. These initial iterations serve the purpose of identifying and correcting any errors in the design.

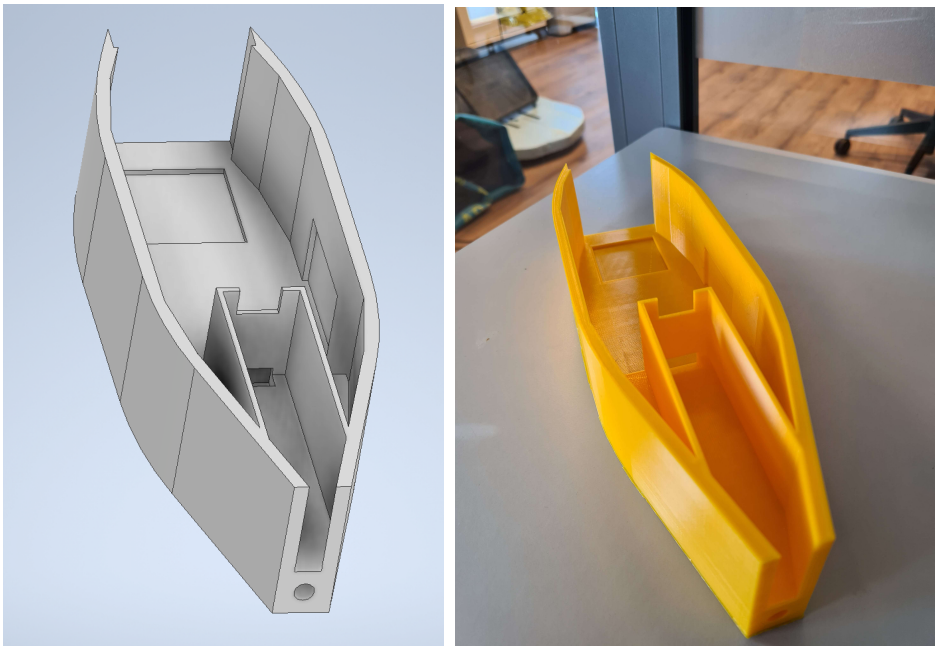

(a) Body 3 sketch (b) body 3 prototype

Figure 3.22: Drone body draft revision three

To accommodate the latest version of the drone body, the motor

holder was further developed, which is illustrated in Figure 3.23. This version's width was reduced, allowing it to fit snugly on the drone body. Additionally, the motor was rotated 45 degrees, effectively reducing the size requirement of the motor holder while still ensuring the motor's stability during flight.

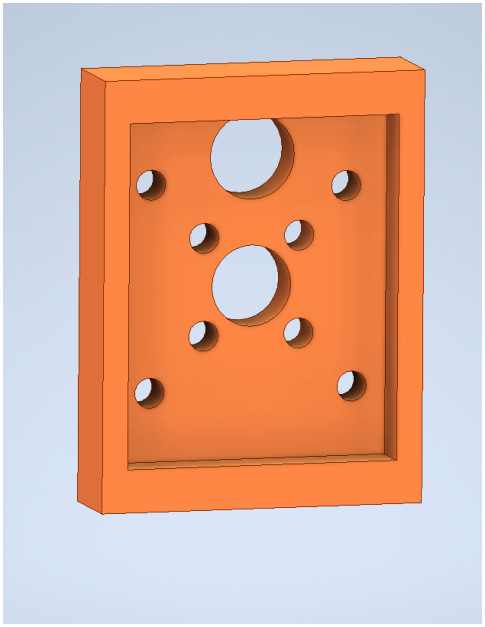

Figure 3.23: Motor holder second iteration

The previous receiver used for testing purposes was a FrSky S6R, which had six inputs for servos, in which the motor and the two servos responsible for the morphing mechanism were connected. The new receiver, which can be found in 3.5, does not have inputs for the servos, so for this new configuration, the servos will be connected directly to the PixRacer.

The previous servos were of the micro variety, measuring 22,3 x 11,8 x 26,3mm and weighing 9 grams. The new servos, found in Table 3.5, have a size of 28,5 x 13,4 x 29mm and a weight of 28,6 grams. In order to accommodate these larger servos and the redesigned drone body, the wing platform had to be redesigned. A sketch and printed version of the new wing platform can be seen in Figure 3.24. In this revision, the servos will be mounted from below due to their increased size. Holes were not designed for the servos, but instead, holes will be drilled to securely attach the servos with screws rather than glue. Protrusions have been included to the front and back of the wing platform, which will function as attachment points for the rubber band. Observed in the intended space for the sliding base, room for a 5mm carbon fiber rod has been allocated where it will be attached with glue, extending through the entire wing platform and out to the edges of the sliding base. This carbon fiber rod is included to increase the structural integrity of the sliding bases. An example of how this carbon fiber rod will be installed can be seen in Figure 3.24c. As can be seen from

this figure, a space for the carbon fiber rod was also made in the sliding base.

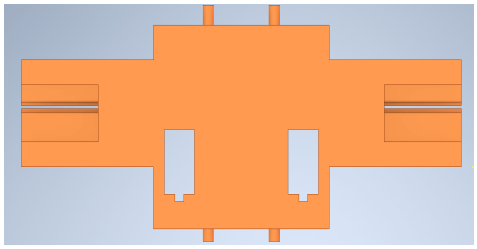

(a) wing platform sketch

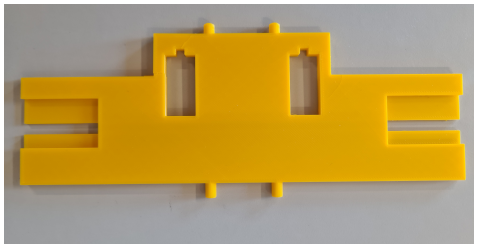

(b) wing platform prototype

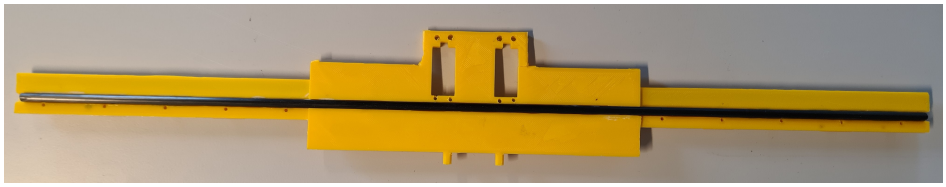

(c) Carbon rod installed

Figure 3.24: wing platform revision three

In this revision, the most significant change is the new design of the drone's body. Given the previously established functionality of the morphing mechanism and already having an experimental proof of concept, the morphing mechanism was not assembled. Instead, the focus was placed on ensuring that all the additional components required for the PixRacer could fit inside the drone body. By testing with the PLA version of the body, it was confirmed that all of the components related to the PixRacer could fit inside the body. Moreover, the redesigned wing platform seamlessly fits the updated body, requiring only minor adjustments, such as premade holes for attaching the servos. The next section will describe these minor adjustments and a print of the body in lightweight PLA.

Table 3.4: Components used for revision three

Component	**Currently used component**
Morphing mechanism Servo	Power HD M8 8.5kg / 0.058s
Tail servos	Dualsky DS395 Digital Micro Servo 1.5kg/0.10s
Motor	Dualsky ECO 2312C V2 960KV 58gram
Battery	3s 2200mAh - 20C - Gens Ace Soaring Mini XT60
Receiver	FrSky R-XSR 2.4GHz Micro Receiver
Flight Controller	Pixracer R15
ESC	Hobbywing SkyWalker 30A ESC
Radio	Taranis X9D

3.3.6 Revision Four

The main objective of this revision revolves around the transition to the new lightweight PLA body. Due to the limited availability of the lightweight PLA printer, several test prints of the new body using regular PLA were made prior to printing it using lightweight PLA. The first version of the lightweight PLA body can be seen in Figure 3.25b, and as can be seen here, it weighs 59 grams. This represents an approximate reduction of 60% compared to the identical body printed using regular PLA, which weighs 150 grams.

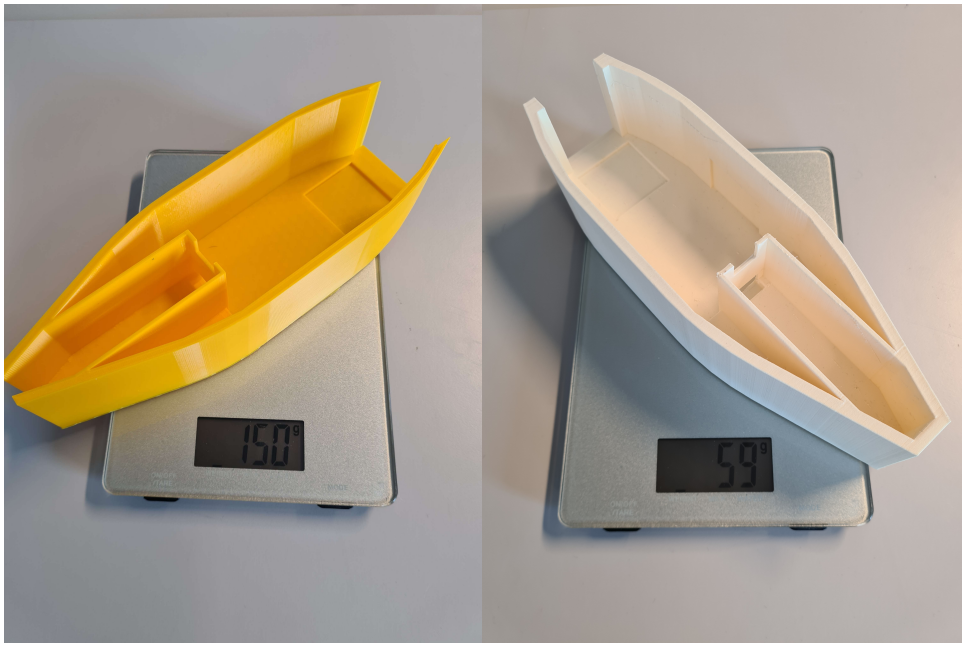

(a) Drone body weight PLA (b) Drone body weight Lightweight PLA

Figure 3.25: Weight difference PLA and Lightweight PLA

With the new lightweight PLA body, the installation of various components for the upcoming test flight began. Not long into the installation, it was revealed that several critical parts were overlooked during the transition to the new body. The first of which was attaching the morphing mechanism, which is currently done through the use of rubber bands. However, with this new body, it was discovered that heat-set threaded inserts could be incorporated into it. These inserts can be used to attach parts such as the motor holder, wing platform, and various covers by using screws instead of rubber bands and glue.

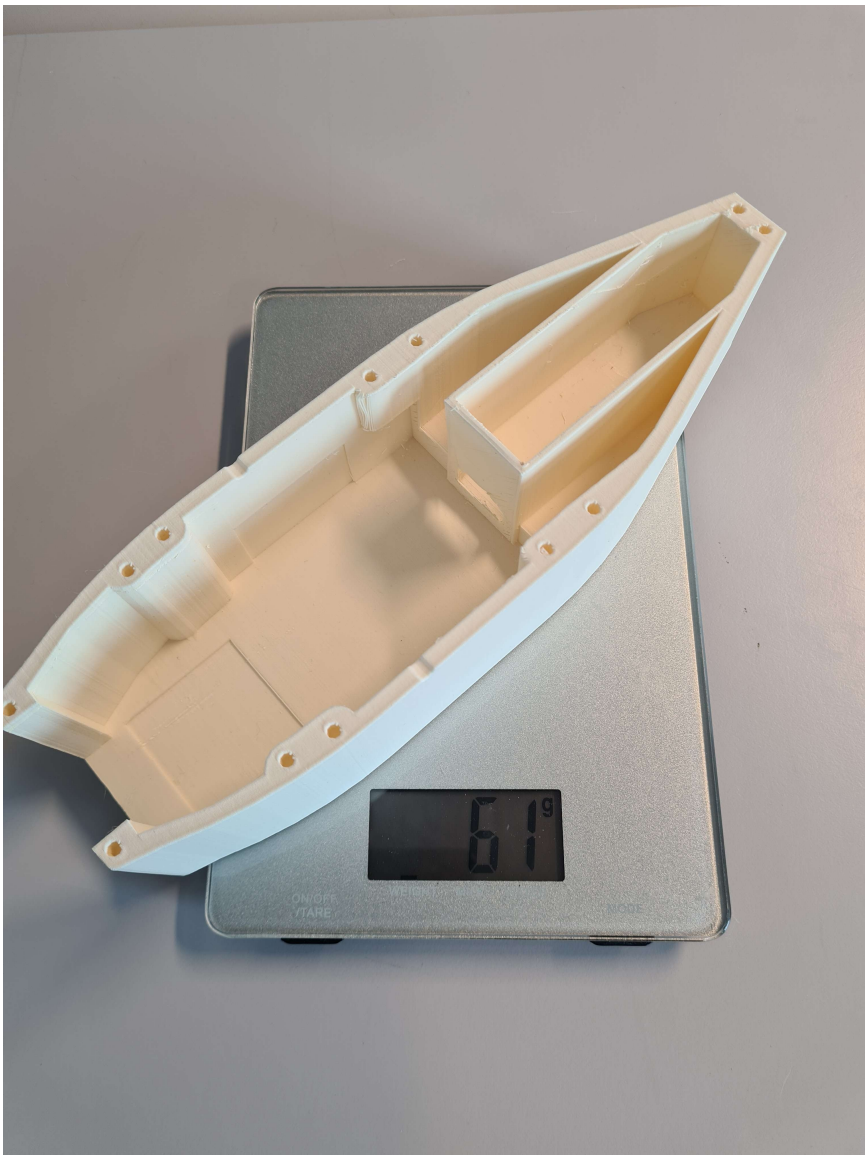

Figure 3.26: Weight of reprinted version of drone body

In order to be able to use the heat-set threaded inserts, the drone body had to be redesigned again specifically for the insertion of them, seeing as they had a length of 6 mm and a diameter of 4.5 mm. For this design, the front of the drone where the motor holder is attached was increased to accommodate the inserts' incorporation. Additionally, on the top of the body, the width was increased in certain areas where the wing platform and the front and back covers will be attached using screws. This new drone body is depicted in Figure 3.26, in which the weight of 61 grams can also be observed. In this new version, the extra space was included to insert twelve of these heat-set threaded inserts, weighing 5 grams, resulting in a new weight of 66 grams for the new body version.

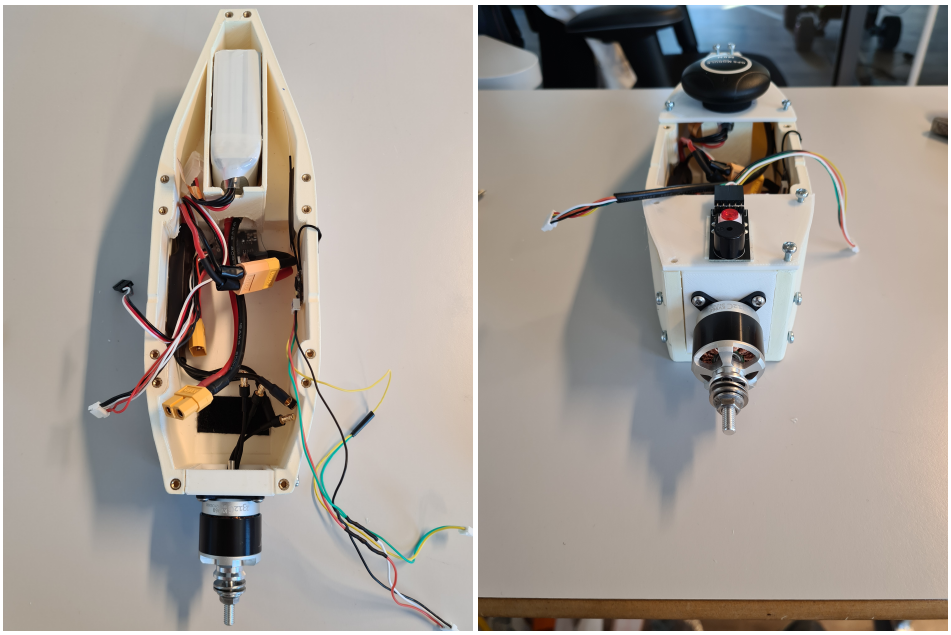

(a) Installing of components

(b) Components installed with covers attached

Figure 3.27: Demonstration of component location with and without coverr

The inserts were inserted into the new body by placing them on a soldering iron and melting them in place, and then all of the required components were installed in their designated place. The insertions can be seen in Figure 3.27a with several components installed in the drone. The components that have been successfully installed in this figure are the ESC, which has been attached in its designated place using double-sided tape, the battery, which is inserted into the back of the drone, and a piece of velcro, which will keep the PixRacer in place behind the motor. Figure 3.27b shows the screws securing the motor holder and the covers at the drone's front and back. Additionally, on the front cover, the safety switch has been installed so that it is possible to arm and disarm the drone safely. Furthermore, the GPS has been positioned on the back cover in the only remaining space outside the drone body.

After completing the assembly, testing of the morphing mechanism with the new servos began. Remarkably, the servos transitioned to a withdrawn position in under 0.5 seconds from a fully extended position. Nevertheless, it was discovered that the air-tight material attached to the feathers contributed to a considerable amount of friction as they overlapped during the folding process. Upon further inspection, this was revealed to be the airtight material at the edges of the feathers coming loose. After several attempts trying to file down the edges to mitigate this issue, it was decided to redesign the feathers.

Figure 3.28: Feather rev 4

Showcased in Figure Figure 3.28 is the redesigned feather weighing 12 grams. However, this version has removed the necessity for air-tight material as the entire feather has been printed using PLA. Furthermore, the length of the feather has been increased again, with the previous version being approximately 160mm long and the new version measuring approximately 205mm. The edges of the feather have also been slanted to facilitate a smoother folding process.

Figure 3.29: wing cover revision four

With all of these modifications, it was decided to redesign the wing cover using a pre-existing symmetrical airfoil. This symmetrical airfoil was used to create a wing cover that covered the wings and extended all the way to the body, covering the front section of the wing platform. Figure 3.29 offers a visual representation of the redesigned wing cover installed on the drone. Given that every alternate feather has an elevated base, some washers were 3D-printed to place atop the non-elevated feathers, ensuring

the wing cover puts even pressure on all of the feathers, maintaining a consistent position.

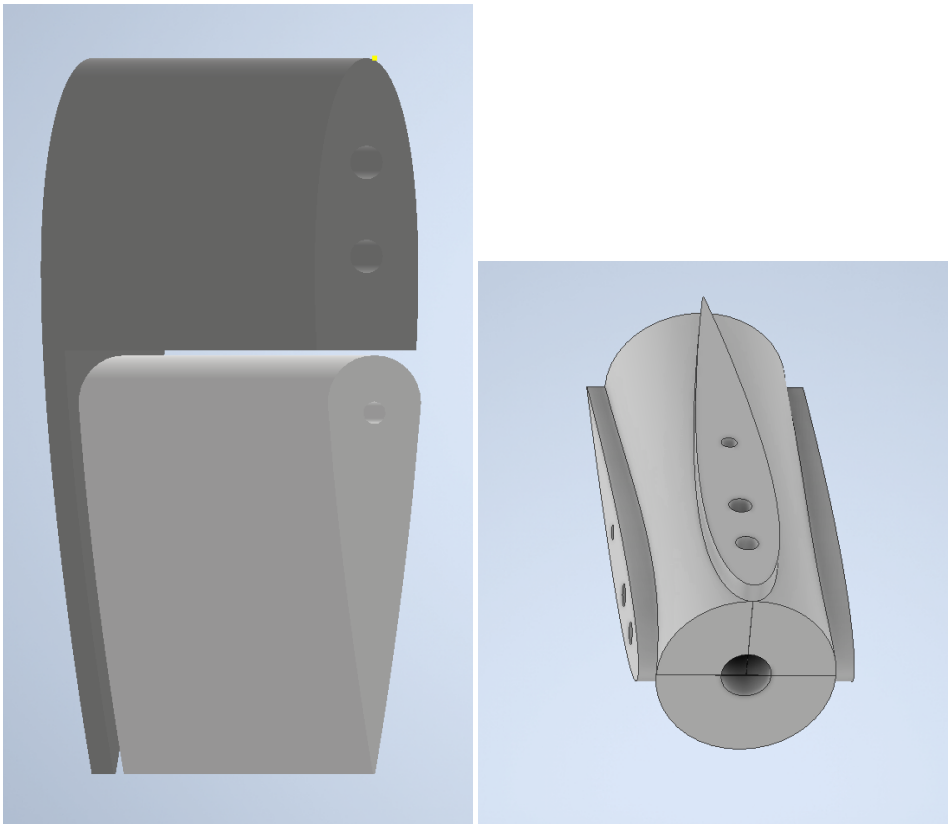

(a) Rudder and elevator (b) Tail end piece

Figure 3.30: Tail components

Initially, the plan was to make the drone's tail primarily out of foamboard. Nevertheless, following the successful fabrication of the drone body using lightweight PLA, it was decided to utilize the same material for the rudder and elevator. The tail structure comprises a rudder and elevator, which will be attached at the end of a carbon fiber rod attached to the drone body. A depiction of the tail mount, designed to be attached to the carbon fiber rod, can be seen in Figure 3.30b accompanied by a sketch of the rudder and elevator. The rudder and two elevators will be attached to this tail mount. Showcased in Figures 3.31 is a visual representation of the tail assembly when installed from the drone. As can be seen from the figures, each moveable surface has a corresponding servo responsible for moving that surface, with the cables securely fastened to the carbon fiber rod using strips.

The stationary pieces of the rudder and elevator are attached using two 3mm carbon fiber rods, with small pieces of double-sided tape utilized to ensure they stay in place. The moveable pieces are attached with a long 2mm carbon fiber rod, which extends from the top of the stationary pieces into the tail mount to give it some additional security. Furthermore, the

servos are attached to the stationary pieces using double-sided tape.

The drone has a wingspan of 52.5 cm at the tip of the feathers and 55cm at the back of the feathers. With the feathers in their resting position, the approximate area of the five feathers, disregarding any overlap, is $344,72cm^2$. With this information, the total area of the feathered area or the wing area of the drone can be calculated and came out to be $689,44cm^2$. As mentioned in Section 2.3.6, general guidance for sizing the rudder and elevator makes the rudder 9-10% of the wing and the elevator 18-25% of the wing area. To simplify the tail design, it was decided to generalize the elevator and the rudder size, making them the same size. Some notable measurements of the general design are a chord of 68,6cm, a span of 100cm, and a thickness of 10,3cm.

Given that the drone being developed is not a conventional fixed-wing drone, it was decided to increase the size of the elevator and rudder due to the tail being mounted slightly lower than initially intended. Taking the average of the recommended sizes, the recommended area for the elevator and rudder can be seen in Equations 3.1 and 3.2. The designed rudder has an area of approximately $71,57cm^2$, which is approximately 10.38% of the wing area. The area of the elevator is twice that, resulting in a total area of $143,14cm^2$, which is approximately 20.75% of the wing area.

$$\begin{aligned} \text{Elevator\_Area} &= 0.15 \times \text{Wing\_Area} \\ \text{Elevator\_Area} &= 0.15 \times 689.44\,\text{cm}^2 \\ \text{Elevator\_Area} &\approx 103.42\,\text{cm}^2 \end{aligned} \tag{3.1}$$

$$\begin{aligned} \text{Rudder\_Area} &= 0.075 \times \text{Wing\_Area} \\ \text{Rudder\_Area} &= 0.075 \times 689.44\,\text{cm}^2 \\ \text{Rudder\_Area} &\approx 51.71\,\text{cm}^2 \end{aligned} \tag{3.2}$$

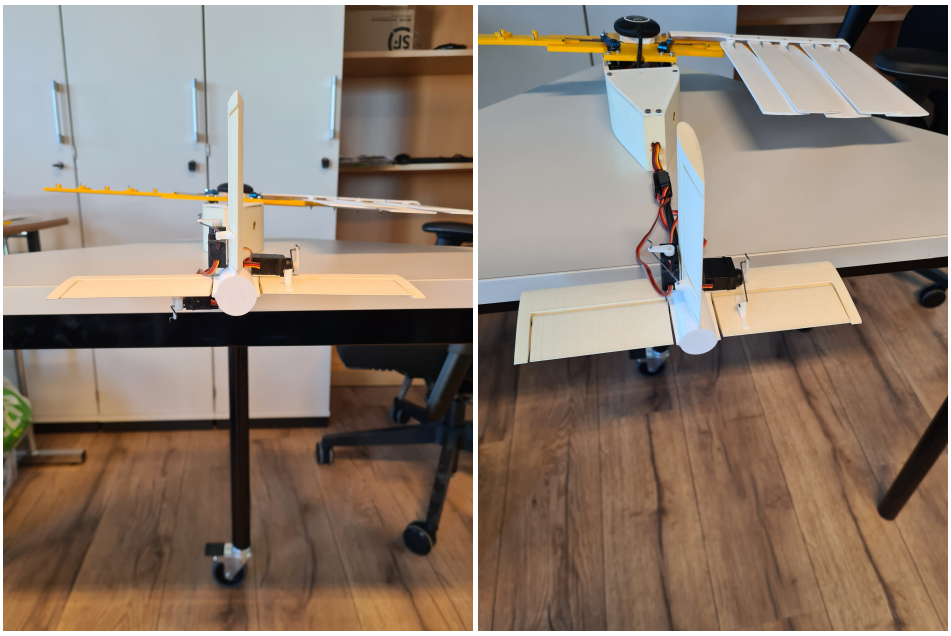

(a) Rudder and elevator (b) Tail end piece

Figure 3.31: Tail installed

With all the modifications described in the section implemented, a complete assembly of the drone can be seen in Figure 3.32. The current weight of the drone is approximately 950 grams, which includes a 3-cell LiPo battery weighing 147 grams. The weight of the drone, excluding any batteries, totals 803 grams. Furthermore, the only notable adjustment that has yet to be described is the new position of the GPS, and it is no longer located on the back cover. Instead, it has now been affixed to the GPS mount attached between the servos on the wing platform.

Figure 3.32: Drone revision four assembled

Upon completing the drone's assembly, the functionality of the morphing mechanism was verified along with the rudder and elevators mounted on the tail. Nonetheless, because of how the servos are mounted, they required additional calibration within Mission Planner to ensure they functioned as intended during flight. Figure 3.44 showcases the range of each servo. Furthermore, servo 1 (assigned to the right wing) required additional adjustments within the radio (Taranis X9D) system to achieve the desirable minimum range, as Mission Planner's limitations restrict a minimum range below 800.

Building upon the successful implementation of the adjustments in

this section, a fully functional drone ready for test flights has now been achieved. The upcoming test will provide valuable insight into the drone's capabilities. This test flight will be briefly described in the following section and described in detail in Section 4.3.1

Table 3.5: Components used for revision four

Component	Currently used component
Servo	Power HD M8 8.5kg / 0.058s
Tail servos	Dualsky DS395 Digital Micro Servo 1.5kg/0.10s
Motor	Dualsky ECO 2312C V2 960KV 58gram
Battery	3s 2200mAh - 20C - Gens Ace Soaring Mini XT60
Receiver	FrSky R-XSR 2.4GHz Micro Receiver
Flight Controller	Pixracer R15
ESC	Hobbywing SkyWalker 30A ESC

3.3.7 Revision Four Test Flight

The initial test flight was conducted using the finalized prototype of the fourth revision of the drone after all necessary configurations were done. With the landowner's permission, the test flight was performed in a remote location with no obstacles nearby. Figure 3.34 shows the prepared setup with the drone, laptop, and radio controller. A pre-flight checklist was reviewed to verify that everything worked as intended.

- Check battery voltage in Mission Planner
- Check GPS (amount of satellites) in Mission Planner
- Check radio connection (verify the radio is connected to the drone)
- Verify that the drone is unarmed
- Test wing-folding
- Test elevators
- Test rudder
- Test motor

For this test flight, an APC 10x7E propeller was used with a 3-cell battery and the Dualsky 2312C 960kv motor. Furthermore, as seen from Figure 3.33, this combination gives the drone a maximum thrust of 1074g [10].

Voltage (V)	Propeller (RPM)	Throttle (%)	Current (A)	Volage (V)	el. Power (W)	Efficiency (%)	Thrust (g)	Spec. Thrust (g/W)
11.1V (3S LIPO)	**10x5E**							
	3000	32	0.7	11.1	7.6	76.5	121	15.8
	3600	39	1.2	11.1	12.7	79.4	174	13.7
	4200	46	1.8	11	19.8	80.8	237	12
	4800	54	2.7	11	29.4	81.4	310	10.5
	5400	61	3.8	11	41.8	81.5	392	9.4
	6000	69	5.3	10.9	57.5	81.3	484	8.4
	6600	78	7.1	10.9	76.9	80.9	586	7.6
	7200	86	9.4	10.8	100.6	80.3	697	6.9
	7800	96	12.1	10.7	128.9	79.7	819	6.3
	8058	100	13.6	10.7	143.8	79	873	6.1
	10x7E							
	3000	33	1	11.1	10.5	77.9	170	16.1
	3500	39	1.5	11.1	16.4	79.3	231	14.1
	4000	46	2.2	11	24.3	79.8	301	12.4
	4500	52	3.2	11	34.6	79.8	381	11
	5000	59	4.4	11	47.7	79.5	471	9.9
	5500	66	5.9	10.9	63.9	78.9	570	8.9
	6000	74	7.8	10.9	83.6	78.3	678	8.1
	6500	82	10.1	10.8	107.4	77.5	796	7.4
	7000	90	12.8	10.7	135.5	76.7	923	6.8
	7500	99	16.1	10.6	168.5	75.9	1059	6.3
	7553	100	16.6	10.6	173.8	75.4	1074	6.2

Figure 3.33: Motor one thrust, Figure from [10]

Once the pre-flight checklist was completed, the drone testing commenced. A throwing start is necessary as the drone does not have landing gears. Unfortunately, the first test flight concluded with a crash landing approximately 4 seconds in, during which the drone performed an unintended backflip. The only damage to the drone due to the crash was a broken left wing. The backflip was caused by a misaligned center of gravity, causing the front of the drone to pitch upward instead of remaining stable. Additionally, a rather severe lacking in the pre-flight checklist was discovered and added to the new checklist in addition to a few other mission points that will be described in 3.3.9.

Figure 3.34: Preperations for first test flight

3.3.8 Revision Five

Due to the outcome of the test flights in Section 4.3.1, the primary focus of this revision is to address the misaligned center of gravity. As showcased in Figure 3.35, the pre-designated battery position was removed, and the Pixracer shifted towards the rear. Relocating lightweight components further back allowed for repositioning the battery towards the front of the drone, effectively moving the center of gravity forward. The figure mentioned above also highlights the newer, more robust servo attachments and the new GPS position.

Additionally, to increase the likelihood of a successful flight, it was decided to upgrade from a 3-cell to a 4-cell battery, providing extra weight and increasing the motor's thrust. However, the current ESC is only rated for 2-3 cell batteries, necessitating a change. The new ESC, compatible with the new battery, can be found in Table 3.7.

As mentioned in section 3.27, the drone weight without any batteries was 803 grams during the fourth revision. Since both the battery and ESC were upgraded for this revision, the total weight of the drone was increased by approximately 72 grams. With these installed, the drone now weighs 826 grams without a battery and 1022 grams with the 4-cell LiPo battery. The test flight with this revision will be briefly presented in the following section with a detailed presentation in Section 4.3.2.

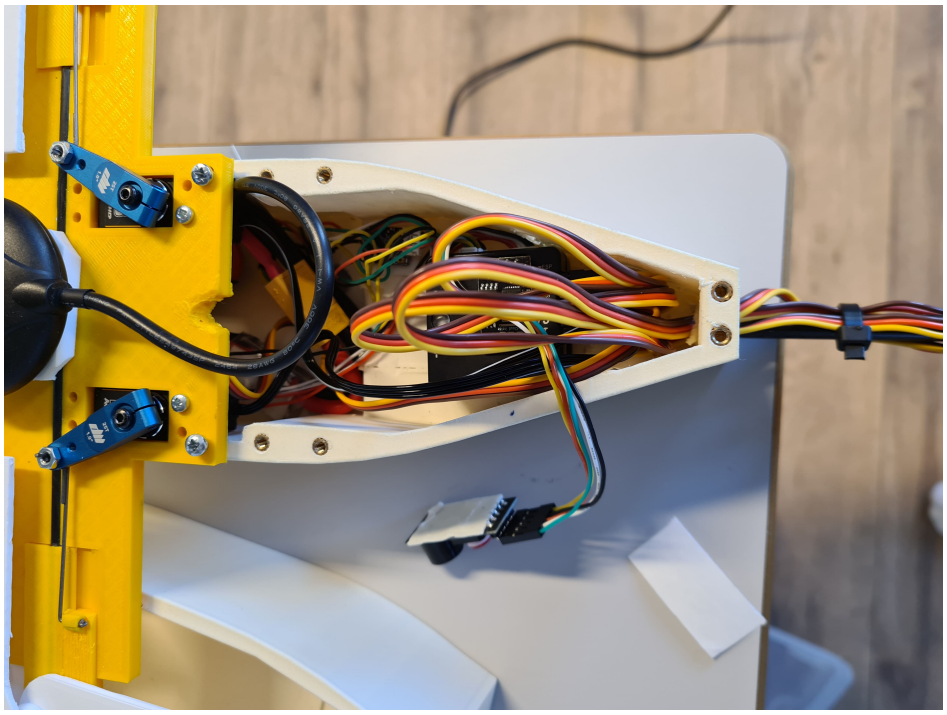

Figure 3.35: Example of relocated components

Table 3.6: Components used for revision five

Component	Currently used component
Servo	Power HD M8 8.5kg / 0.058s
Tail servos	Dualsky DS395 Digital Micro Servo 1.5kg/0.10s
Motor	Dualsky ECO 2312C V2 960KV 58gram
Battery	Tattu R-Line 1800mah 4S 95C FPV Lipo Battery
Receiver	FrSky R-XSR 2.4GHz Micro Receiver
Flight Controller	Pixracer R15
ESC	ZTW Beatles 60A Brushless ESC for 2-6S LiPo

3.3.9 Revision Five Test Flight

With the modifications from revision five implemented, the center of gravity has now been shifted to approximately the middle of the wing platform. The second test flight was conducted at the same location that was described in Section 3.3.7, following the same pre-flight checklist with some additional points, as can be seen in the list below. Due to the previous test flight crash, a soft landing surface was set up roughly 20 meters away from the launch point as a precautionary measure in case the drone encounters any issues during the test flight.

- Check center of gravity
- Check drone for faults

- Check that all nuts are fastened
- Check wind direction
- Check propeller (is it attached correctly and securely)
- Connect Battery
- Check battery voltage in Mission Planner
- Check GPS (amount of satellites) in Mission Planner
- Check radio connection (verify the radio is connected to the drone)
- Verify that the drone is unarmed
- Test wing-folding
- Test elevators
- Test rudder
- Test motor

For the first test, an APC 8x4.7SF propeller was utilized, and since this test was performed with a 4-cell battery, this setup provided the drone with a maximum thrust of 1072 grams. The drone was deliberately launched in a more horizontal direction rather than an upward trajectory to increase the likelihood of it landing on the soft surface. The first attempt resulted in the drone generating an insufficient amount of lift and barely missing the soft landing surface, thus breaking the propeller upon impact.

During the second attempt, since the 8-inch propeller broke, An APC 10x5E propeller had to be used, which has no documented maximum thrust as it is meant for 3-cell batteries. The drone was launched in a more upward trajectory in an attempt to achieve flight. Unfortunately, the drone could not generate enough lift to remain airborne but managed to land on the soft surface successfully. However, during the landing, the stationary part on both elevators broke in the middle, and one servo was damaged.

3.3.10 Revision Six

Building upon the issues discovered in Section 3.3.9, this section will attempt to solve the problem of the insufficient amount of lift generated. The most apparent solution to this problem is to increase the surface of the wings. This will be done in two parts, and the first part is to add an extra feather on each wing, effectively increasing the area of each wing from $344,72cm^2$ to $412,35cm^2$.

Additionally, an extra surface will be added to the wing platform, which will cover the previously open space between the fuselage and the first feather. A sketch of the new wing platform design can be seen in Figure 3.36. Each of these new surfaces increases the area of the wings by $99,95cm^2$, thus increasing the total area of the wings from $689,44cm^2$ to

1 024, $6cm^2$, not including the extra area gained from the redesigned wing cover.

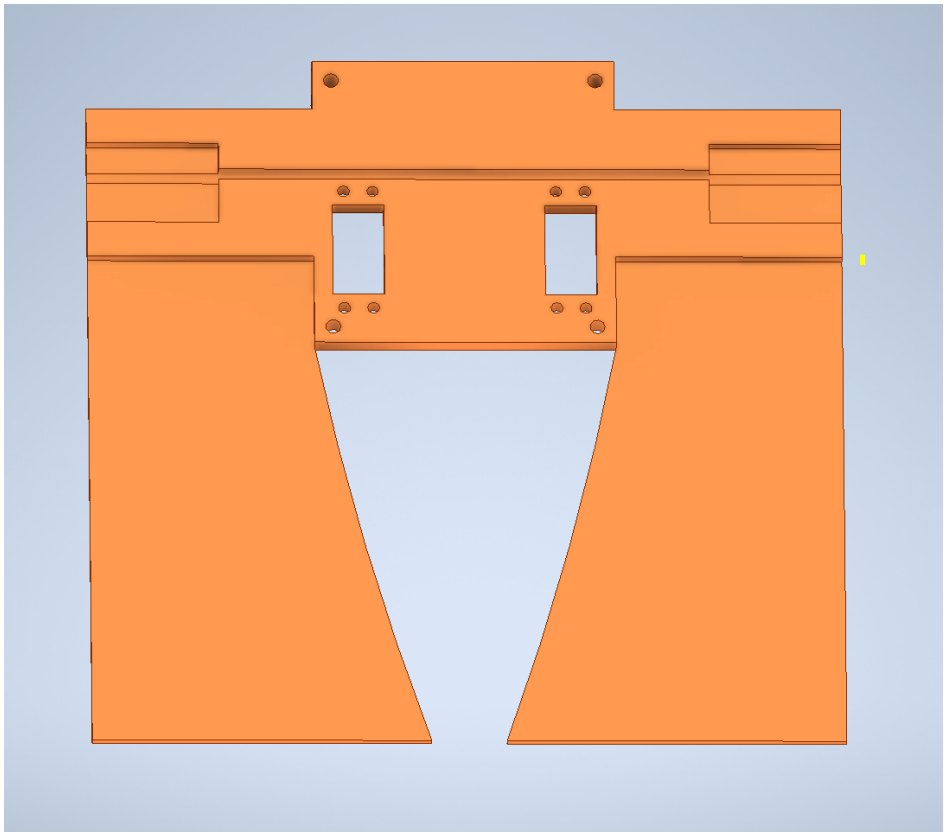

Figure 3.36: Wing platform revision six

In addition to increasing the area of the wings, it was also decided to increase the angle of attack, as the wings were previously mounted at a 0-degree angle. As displayed in Figure 3.37 under the frontmost screw holes, some pillars have been added to enable mounting at an angle. By mounting the wing platform using these new pillars, it is now mounted at a 6-degree angle. In order to accommodate the new angled wing platform, the body was also redesigned, as when the feathers are folded in, they would collide with the body. This was fixed by lowering the rear of the body, also illustrated in the previously mentioned figure. Furthermore, since the body was already being redesigned, the hole in which the carbon fiber rod for the tail is attached will be moved higher to elevate the tail.

Figure 3.37: Body and wing platform demonstration

As illustrated in Figure 3.38, the two outmost feathers on the right wing have been replaced with bright orange feathers. Furthermore, the wing cover on the right side now also exhibits an orange hue. These colors were deliberately picked in order to facilitate easy identification of the drone's orientation during flight, based on the distinct colors.

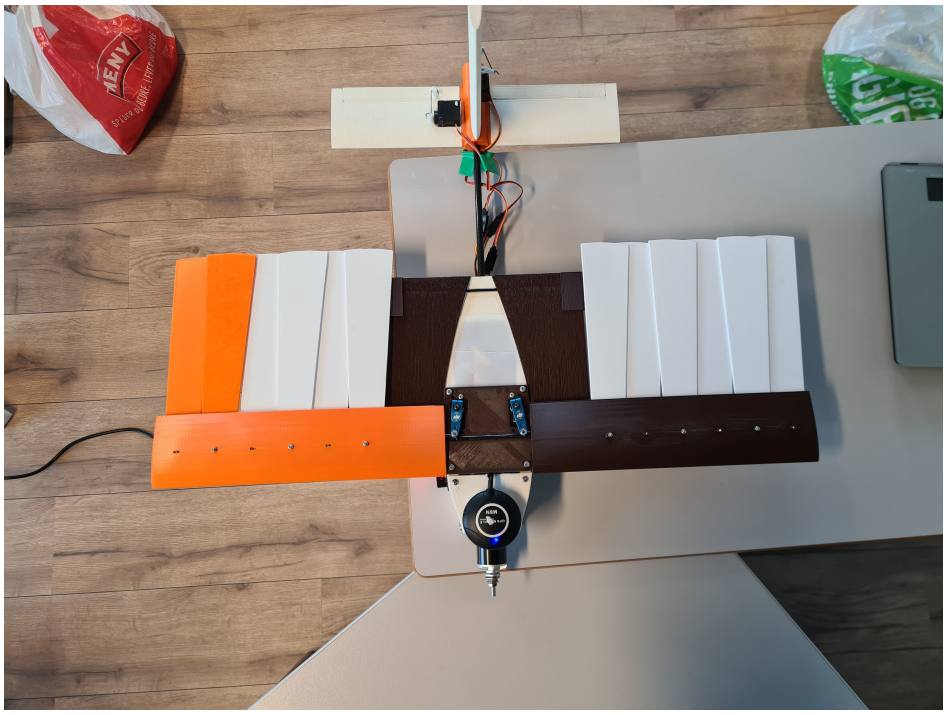

Figure 3.38: Revision six

In an attempt to further increase the lift, the wing cover was also redesigned. The previous wing covers had a softer front to split the air more efficiently. The new wing covers were made using a NACA-0012 airfoil template by extending it from the body to the tip of the sliding base. Using this template allowed for the design of a wing cover where the leading edge of the airfoil was kept, as well as approximately 60-70% of the airfoil itself, before cutting the trailing edge to allow for the feathers to fold in between it.

(a) Revision six complete assembly

(b) Revision six complete assembly

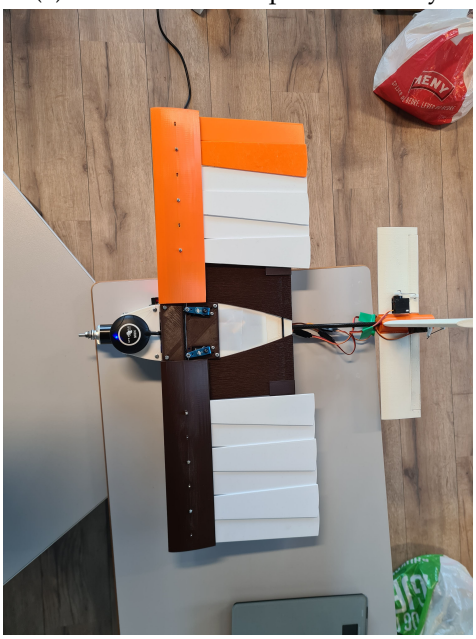

(c) Revision six complete assembly

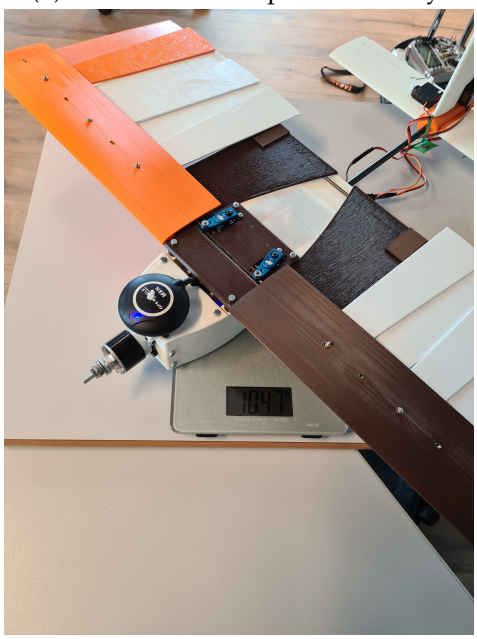

(d) Revision six complete assembly weight

Figure 3.39: Revision six complete assembly

The rudder and elevators developed for this revision were made prior to the updated wing cover version. Therefore the wing area used for their design only incorporates a wing area of $1,024.6cm^2$, which was calculated earlier in this section. The general guidance dimensions outlined in Section 2.3.6 were used as a recommendation while designing the rudder. However, considering a rudder size between 9-10% appeared excessive, it was decided to create it using 7.5% of the total wing area. Utilizing

a NACA-0012 airfoil, the total area of the rudder equaled 76.85cm^2, as demonstrated in the equation below. This rudder has a chord length of 8.78cm and a height of 17.52cm.

$$\begin{aligned} \text{Rudder\_Area} &= 0.075 \times \text{Wing\_Area} \\ \text{Rudder\_Area} &= 0.075 \times 1024,6\,\text{cm}^2 \\ \text{Rudder\_Area} &\approx 76.85\,\text{cm}^2 \end{aligned} \tag{3.3}$$

Like the previous tail design, the elevator was divided into two parts, split in the middle by the tail mount. Once again, it was decided to deviate slightly from the recommended range of 18-25% and instead, decided to make the combined elevator size 15% of the wing area. Using the same wing area as the rudder to calculate the size and also using a NACA-0012 airfoil, the total size of both elevators combined equaled 153.57cm, as demonstrated in the equation below. This resulted in each elevating having a total size of 76.79cm. The elevators feature a chord of 6.05cm and a height of 13.58cm. The finished product of the elevators and rudder, installed on the new tail mount, can be viewed in Figure 3.40.

$$\begin{aligned} \text{Elevator\_Area} &= 0.15 \times \text{Wing\_Area} \\ \text{Elevator\_Area} &= 0.15 \times 689.44\,\text{cm}^2 \\ \text{Elevator\_Area} &\approx 103.42\,\text{cm}^2 \end{aligned} \tag{3.4}$$

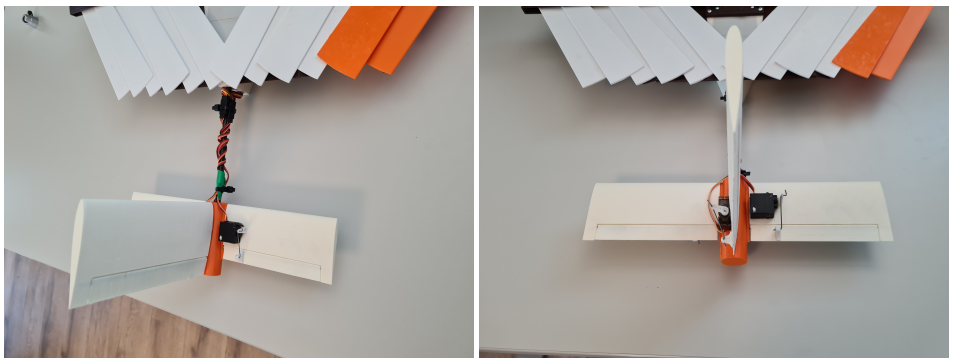

(a) Tail revision 6 (b) Tail revision six

Figure 3.40: Tail installed

Since the drone has undergone numerous changes in the sixth revision, the weight has also increased. A finished drone assembly and base weight without any batteries can be seen in Figure 3.41, resulting in an increase of approximately 88 grams from the fifth revision. The majority of this weight increase results from two additional feathers and the redesigned version of the wing cover.

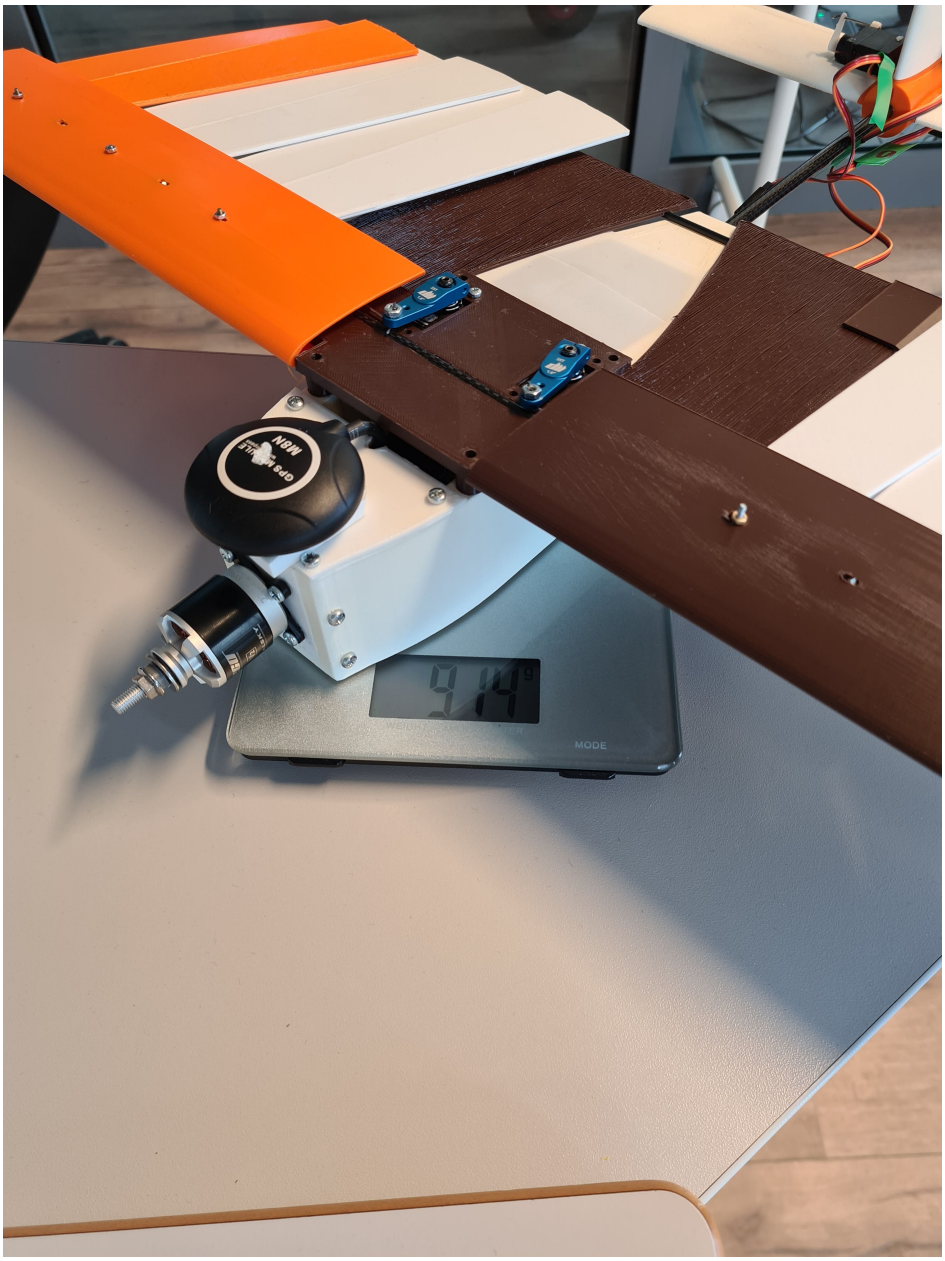

Figure 3.41: Revision six base weight

Table 3.7: Components used for revision Six

Component	Currently used component
Servo	Power HD M8 8.5kg / 0.058s
Tail servos	Dualsky DS395 Digital Micro Servo 1.5kg/0.10s
Motor	Dualsky ECO 2316C V2 980KV 72gram
Battery	Tattu R-Line 1800mah 4S 95C FPV Lipo Battery
Receiver	FrSky R-XSR 2.4GHz Micro Receiver
Flight Controller	Pixracer R15
ESC	ZTW Beatles 60A Brushless ESC for 2-6S LiPo

3.3.11 Revision Six Test Flight

The test flight for the sixth revision of the drone was performed in a remote area in Lommedalen to maintain a safe distance from anything. For this test flight, instead of using only one battery, the goal is to test the performance of different sorts of batteries and propellers in an attempt to figure out if the extra weight of a 4-cell battery outweighs the extra thrust gained. So for this test flight, the attempt will be split into sections based on the battery and propeller used.

The first attempt will be performed with a 2200mAh 3-cell battery with a C-rating of 20 and an APC 11x7E propeller, giving the drone a thrust of 1512 grams at full throttle [9].

The first attempt resulted in a quick crash shortly after the launch. The crash was determined to be partly caused by the pilot. Due to this, an overview of the flight will be presented in Section 4.3.4.

3.3.12 Revision Seven

As a result of the outcomes of the sixth revision's test flight, it was decided to print a new drone body using standard PLA to get an additional test flight. The Assembled drone, with its updated body, can be seen in Figure 3.42. The overall weight of the drone increased due to replacing the lightweight PLA body with regular PLA resulting in a total weight of 1209 grams when equipped with a 4-cell battery and an APC 9x6E propeller.

Figure 3.42: Revision seven

3.3.13 Mission planner setup

For this project, a Taranis X9D radio controller was used. In order for it to function correctly, a radio calibration is necessary. When calibrating a radio in MissionPlanner, it detects the minimum and maximum output possible from each assigned source. As depicted in Figure 3.43, this range is displayed at the red lines with all the accepted ranges in the pop-up box.

Figure 3.43: MissionPlanner Radio Settings

Since most of the servos used for this thesis are ready to go out of the box, they require additional adjusting and fine-tuning to function as desired. This adjustment can be made using a combination of MissionPlanner and the output calibration in the Taranis Radio. This method section consists of several different revisions of the drone. Because of this, each revision has unique settings, but this section will only cover the last revision, revision seven. As displayed in Figure 3.44, each servo's minimum and maximum output can be observed.

In order to have the servos responsible for the feathers mounted the same direction, several adjustments had to be made to the radio. The first adjustment performed on the radio is adjusting the output of the fifth servo in the previously mentioned figure or the right wing. The output range of this servo is modified from the regular 0% -> 100% to -100% -> 100% allowing the servo responsible for the right wing to move further, thus giving the servo a broader range of motion.

The second adjustment in the radio is an adjustment of the weight for both the right and the left wing. The weight of both servos responsible for

adjusting the wings was reduced from 100% to 50% to allow for a smoother transition and reduce the rapid movements that occurred during minor radio adjustments.

Figure 3.44: MissionPlanner servo settings

With the addition of the external GPS, the drone has two functioning compasses. These compasses can be seen at the top of Figure 3.45, with the external compass having the dev type "QMC5883L" and being positioned first in the list. The second compass with dev type "LIS3MLD" is the internal compass from the PixRacer.

Furthermore, since the PixRacer is secured using double-sided tape, it is not positioned 100% leveled. The compass that functions as the primary compass is the one located in the external GPS. However, since there are two compasses connected and calibrated, the option of using the PixRacer compass functioning as a backup in case the external GPS suddenly stops working mid-flight will be utilized.

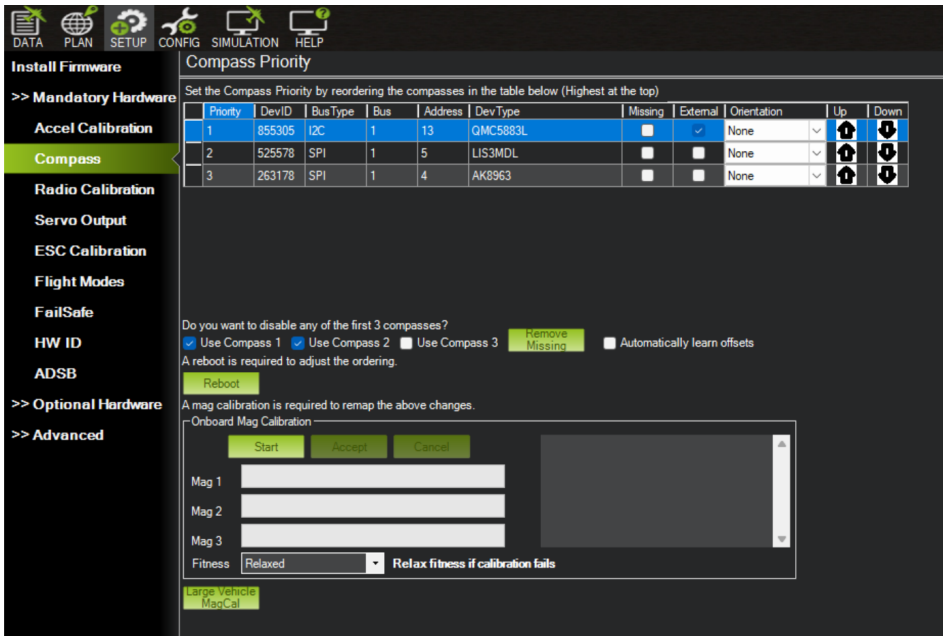

Figure 3.45: MissionPlanner compass settings

With the Taranis having six switches capable of switching between three different levels, one of these can be used to change flight modes during flight. As shown in Figure 3.46, three different flight modes have been selected: manual, Fly by wire A (FBWA), and Stabilize. Using the manual mode, the only inputs that affect the drone are the ones performed by the pilot. In FBWA, a preset maximum roll and pitch angle can be set, not allowing the plane to roll or pitch further than the angles determined. This flight mode is ideal for inexperienced pilots as it significantly reduces the risk of rolling the drone too far or reaching a pitch degree, causing it to stall. The last mode, stabilize, uses essential stabilization in order to keep the plane level if the pilot performs no actions.

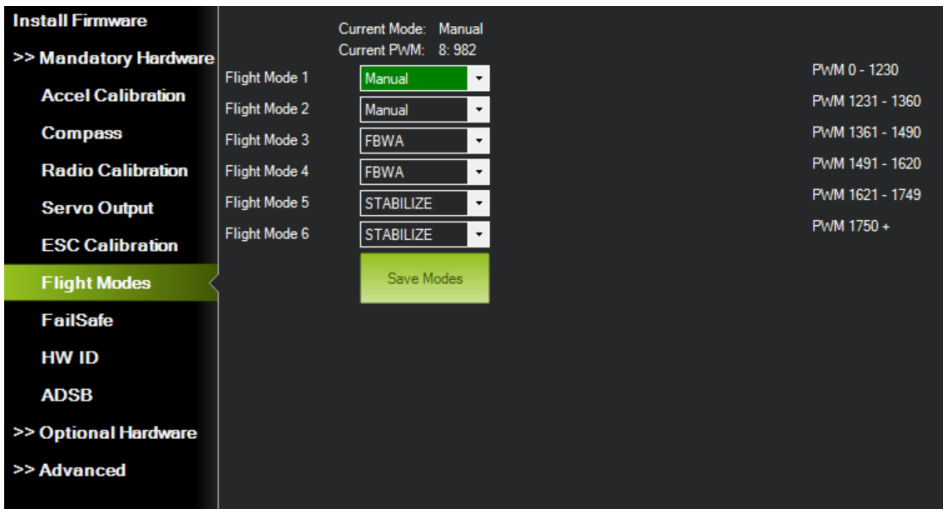

Figure 3.46: MissionPlanner flight modes

Figure 3.47 showcases what the main screen of MissionPlanner looks like, with the drone's orientation and most critical information in the top left window. Below that window is a customizable pre-flight checklist, including important information like battery percent, number of satellites, and telemetry signal. The main screen in the middle displays the drone's heading on a map, and custom waypoints will also be displayed here if used.

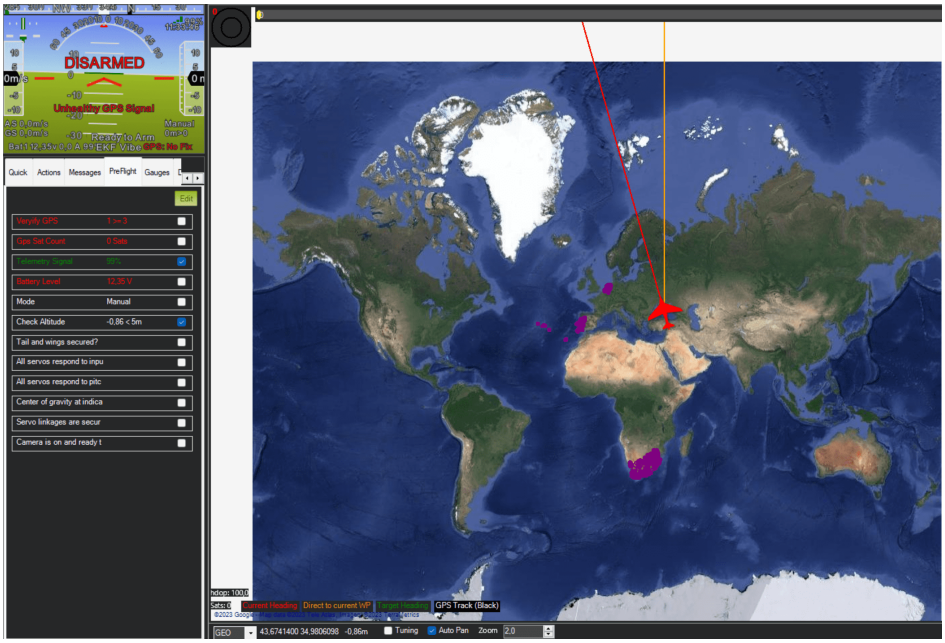

Figure 3.47: MissionPlanner main screen

Chapter 4

Results

In this chapter, the results will be presented.

4.1 Revision overview

In this section, a recap of the most significant changes done to each revision of the second morphing mechanism as well as the results of the morphing mechanism for each revision is provided.

Revision 0 (initial prototype) The initial prototype of the second morphing mechanism displayed the fundamentals behind the idea of the morphing mechanism. However, due to several components still requiring further modifications, it was never adequately tested.

Revision 1 In the first revision, the motor holder was introduced in order to keep the motor in a fixed position at all times. Additionally, this revision visited the first redesign of the feathers and the sliding base, moving the elevated base that enabled the feathers to fold without colliding from the feathers to the sliding base. During the testing of the morphing mechanism, a reevaluation of the printing techniques used for the sliding rack was necessary due to pins breaking after just a few tests.

Revision 2 In the second revision, the bottom of the drone body and the wing cover, initially made of foamboard, were replaced by redesigned 3D-designed counterparts. The testing also revealed that the servos responsible for the morphing were too weak to fold the wings in a sufficient amount of time.

Revision 3 The majority of changes in the third revision involved incorporating the PixRacer system in the drone and upgrading the servos. The incorporation of the PixRacer necessitated a larger body to house all of the necessary components. A redesigned body was printed in regular PLA to verify that all the components could be fitted. This revision only consisted of redesigning parts with no actual testing of the morphing mechanism, so it was more of a transitional revision.

Revision 4 With an acceptable design of the drone body reached in revision three, a body was printed using lightweight PLA utilizing heat-set inserts to replace the previously used rubberband to attach the morphing mechanism. Due to the new body, several other pieces also had minor

modifications done to fit in the new body. The tests of the morphing mechanism with this revision included the new servos. With them, the speed required to withdraw the feathers fully was reduced from 2 seconds (from revision two) to 0.5 seconds.

Revision 5 Due to the results of the test flight mentioned in 3.3.7, the only changes made to the fifth revision were upgrading and relocating the battery and installing an ESC that could accommodate the new battery.

Revision 6 During the sixth and final revision, the drone underwent several changes in an attempt to increase the amount of lift generated. The wing area was increased by adding another feather on each wing, creating a new wing platform with an additional surface between the body and the innermost feather, and redesigning the wing cover using an airfoil.

4.2 Morphing Mechanism Performance

This section will present key features related to the morphing mechanism.

4.2.1 Total wing area of the drone

As briefly mentioned in Section 3.3.10, the total area of the feathers and the additional surface added onto the wing platform was $1\,024,6cm^2$. However, with the wing cover, the area was increased even further. To calculate this new wing area, a sketch was made in Inventor using drone measurements. The sketch and the area can be observed in Figure 4.1. As can be seen here, the feathers' total area and the wing cover's latest version resulted in an area of $507,07cm^2$. Using the information presented in the previously mentioned section, the extra attachment to the wing platform added $99,95cm^2$ each, a total of $199,99cm^2$. This brings the total wing, with the feathers in their resting position to a total of $1214,13cm^2$

Furthermore, the drone has a wingspan of 60,8cm, with a distance from the leading edge (front of the wing cover) to the trailing edge (furthest back point on the feathers) of 22,8cm. The body has a length of 25cm and a width of 8cm at its widest, with the tail end piece being mounted approximately 14,5cm behind it.

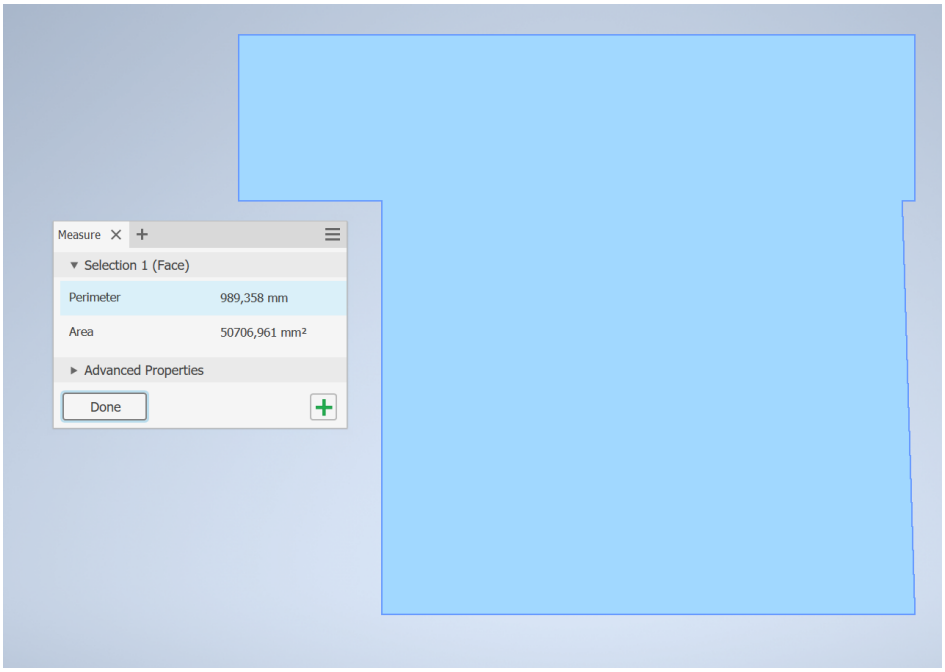

Figure 4.1: Total area of feathers and wing cover

4.2.2 Area that gets reduced

The area calculated in the previous section is when the wings are resting, and the drone is meant to be flying straight. However, when the drone is rolling, the feathers are fully withdrawn. In order to calculate the total area that gets reduced for each wing, measurements were taken with the feathers withdrawn, as can be seen in Figure 4.2. The sides of an irregular quadrilateral were measured to be $13,2cm, 2,4cm, 11,5cm, 16cm$, and an inventor sketch was created to calculate the total area. The total area that gets reduced when the wings are fully withdrawn was $91,74cm^2$, and by dividing the total area of the drone in two, and with the area of one wing being $607cm^2$, thus giving a reduction of approximately 15%.

Figure 4.2: Calculations of reduced area

4.3 Flight/experiments

This section will present each test flight and provide an overview of the flight, provide in-depth information on several factors associated with the flight, and describe any potential to the drone.

4.3.1 Test Flight One

The goal of the first test flight was to evaluate the flight characteristics of the drone and the morphing mechanism during flight. However, approximately 4 seconds into the flight, the drone crashed. The crash occurred due to the drone pitching upwards aggressively, causing it to do a backflip and swiftly crash into the ground. As a result of the crash, the left wing of the drone broke, as can be seen in Figure 4.3.

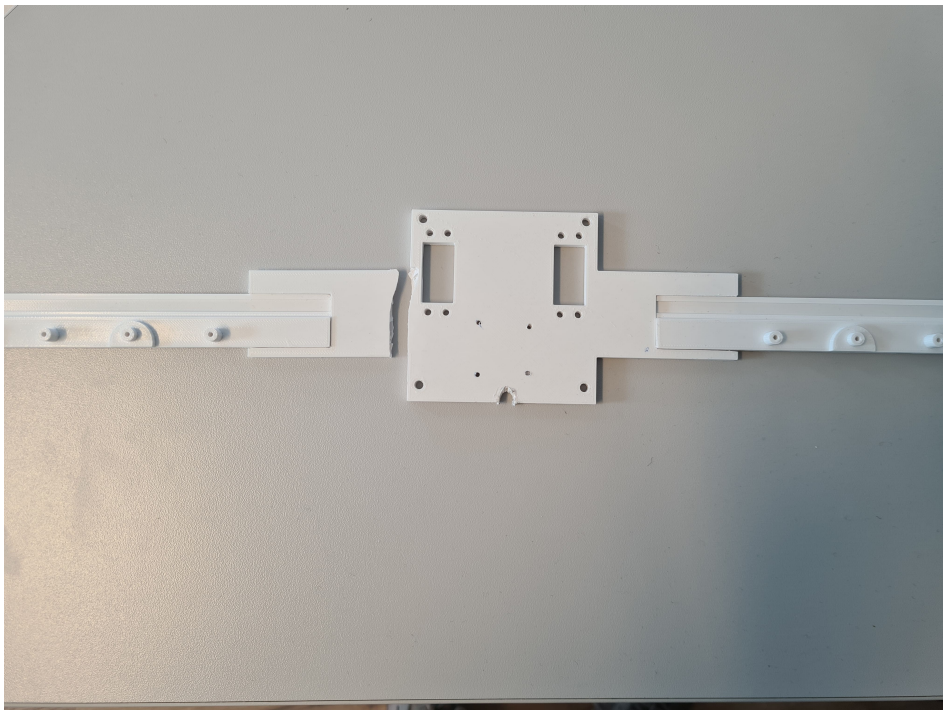

Figure 4.3: Damages from test flight one

4.3.2 Flight Two, Attempt One

For the first attempt of the second test flight, a horizontal launch was utilized in an attempt to assess the drone's capability to fly without causing any damage to it due to the limited height it would reach. For this attempt, an APC 8x6E propeller was used. Launching the drone using a horizontal launch, it crashed into the ground approximately 3 seconds into the flight. This launch method resulted in the drone exiting at a too-low speed, resulting in the drone being unable to generate enough lift to remain airborne. The drone could not climb any higher than approximately 2 meters above the ground, and the crash did not cause any significant damage to the drone. However, one of the props on the propeller broke upon impact with the ground.

4.3.3 Flight Two, Attempt Two

Due to the results of the previous attempt, the drone was now launched in a more conventional upward trajectory, a more commonly used launch method for fixed-wing drones. However, the drone stalled out mid-air and crashed after flying for approximately six seconds.

The consequence of the crash was the front of the drone body, where the motor is located, coming loose. Additionally, both of the stationary pieces of the elevator broke in the middle, and the servo located on the underside of the tail broke in the crash.

4.3.4 Test Flight Three

The third test flight involved several modifications based on information obtained from previous test flights. The drone was again launched in an upward trajectory and stalled out shortly after launch. The damage caused to the drone was similar to that of the second test flight's second attempt, with the front section of the body, where the motor is attached, coming loose.

Figure 4.4 illustrates the drone's position during different timesteps. Each timestep is numbered sequentially, beginning from when it is held by the launcher (number one) to moments before impact with the ground (number six). The second image captures the drone a few moments into the launch, showing the drone slightly tilted to the right, but already in image three, the drone has stabilized and started climbing. The angle at which the drone is climbing in image three is remarkably steep, given the limited speed generated this early in the flight. By image four, the drone begins stalling and rapidly loses most of its speed. Images five and six display the drone completely stalling out and the inevitable plummet toward the ground, unable to recover.

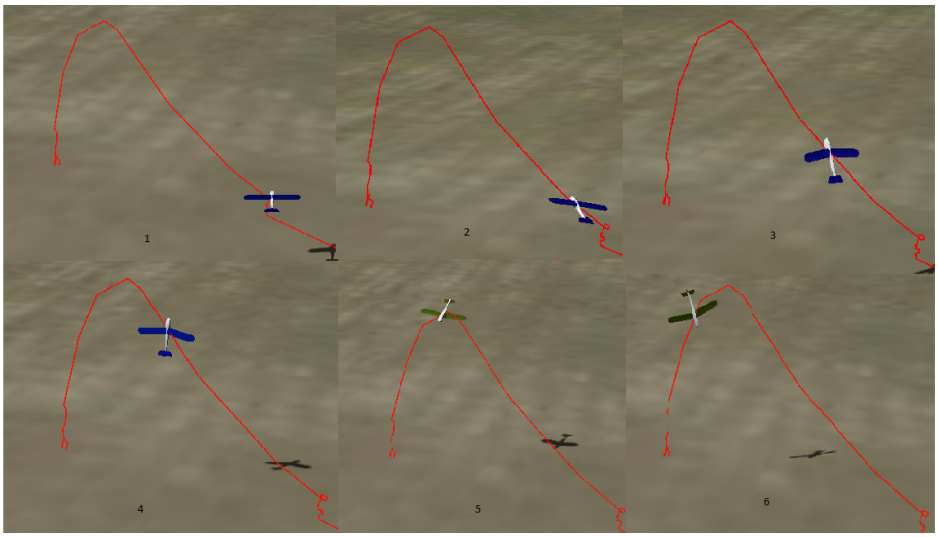

Figure 4.4: Test flight three path

An image of the crash can be seen in Figure 4.5a, and from Figure 4.5b, a further inspection of the damages can be seen with several components removed. As can be seen from the latter figure, the body snapped in half in addition to some other structural damages.

(a) Test flight three crash (b) Damages from test flight three

Figure 4.5: Test flight three crash consequences

4.3.5 Test Flight Four

The fourth test flight consisted of three different attempts, each with a video displaying the flight. These videos can be seen here: Attempt one Video [32], attempt two Video [34], and attempt three Video [33].

A 4-cell battery and an APC 9x6E propeller were used for the first attempt, and this setup provided the drone with a thrust of 1570 grams at maximum throttle [9]. Unlike previous attempts that used manual fight mode, the stabilized flight mode was used for this attempt. Figure 4.6 displays the entire flight path of the first attempt, with the red lines indicating the drone is in manual mode. The orange lines indicate that the flight mode has been switched to stabilized, and it can be seen that this switch occurs slightly before the launch and remains that way throughout the entirety of the flight.

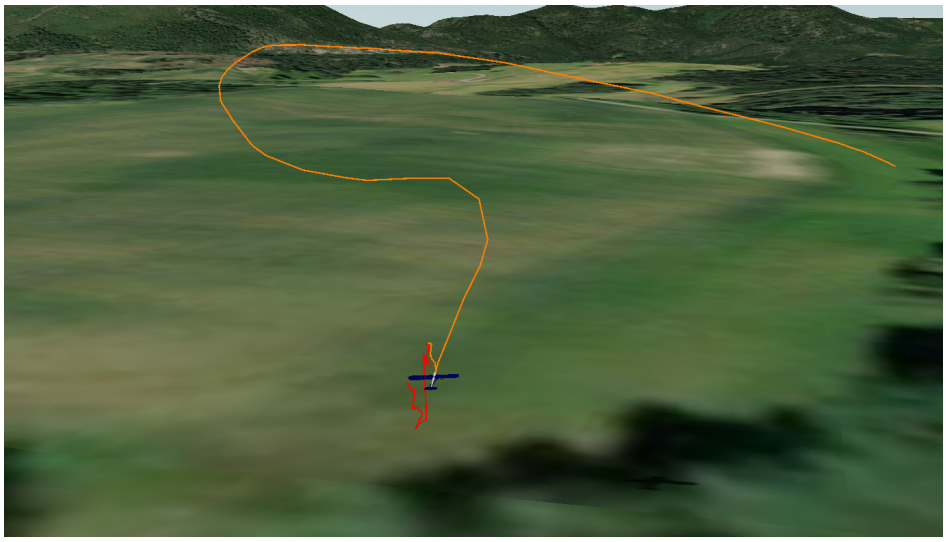

Figure 4.6: Test flight four attempt one - full path

Figure 4.7 presents the drone's position during different timesteps of the flight, arranged in a left-to-right order from the start to the end of

the flight. The figure highlights how the drone rolls in the direction of its turn. Shortly after the launch, the drone started stabilizing using the self-stabilizing feature of the PixRacer and started climbing upon receiving additional inputs from the pilot. However, due to the drone's speed and limited area, a right turn was initiated as the drone would soon be challenging to navigate properly due to the distance between the pilot and the drone. The turn can be observed in the middle row of images, where the drone rolls to the right and begins initiating the turn. Despite this, the pilot attempted a gentle landing due to reducing the thrust and increasing distance to the drone.

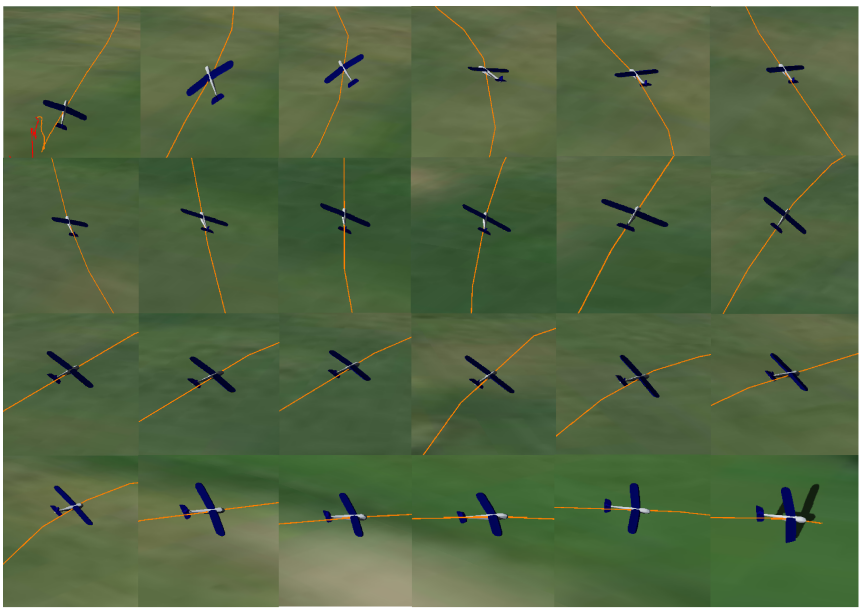

Figure 4.7: Test flight four - attempt one

Some images from the video of the flight described above can be seen in Figure 4.8. The three first images are of the drone shortly after launch and showcase the drone adjusting the wings in order to stabilize. The last image demonstrates the increasing distance from the pilot to the drone.

(a) Attempt 1

(b) Attempt 1

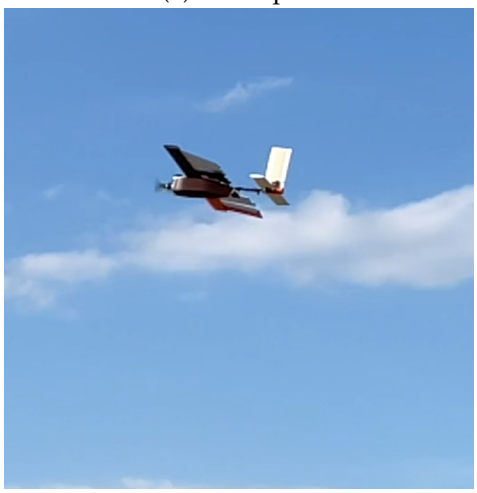

(c) Attempt 1

(d) Attempt 1

Figure 4.8: Images from video of attempt 1

The attempted landing resulted in a relatively soft landing, with the drone reducing its speed gradually. The only damage due to the landing was a broken propeller and a slightly twisted tail, as depicted in Figure 4.9.

Figure 4.9: Test flight four - attempt one crash

In the second attempt, the same 4-cell battery was utilized. However, due to the damaged propeller from the previous attempt, the propeller was replaced by an APC 8x6E. This change led to a decrease in the maximum amount of thrust from 1570 grams down to 1244 grams [9]. The flight path for the second attempt can be seen in Figure 4.10. This figure also includes the travel and downtime between the second and third attempts, which accounts for the additional orange line going past the turning point of its current trajectory. Furthermore, the red lines represent that stabilize mode is active and shows the drone being moved by hand on the ground.

Figure 4.10: Test flight four attempt two - full path

Moments into the second launch, rather than proceeding straight forward, it rotated approximately 45 degrees to the left, as shown in Figure 4.11, which features both the drones position in the flight path as well as an image from the video of the flight, which was filmed from approximately 20 meters ahead of the drone launch. The image from the video demonstrates how the feathers on the right side are fully retracted in order to stabilize the drone.

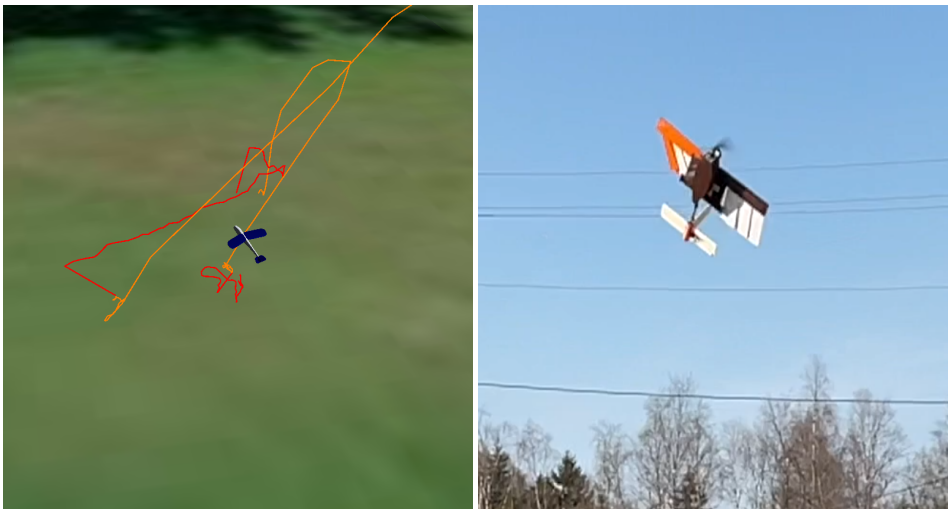

(a) Drone position according to GPS (b) Actual drone position from video

Figure 4.11: Comparison between flight path and image from video

Due to the unexpected behavior at the start of the launch, the throttle was reduced as the drone started flying toward the person filming. Figure 4.12 shows the drone falling toward the camera, attempting to steer away but ultimately resulting in a soft landing causing no damage to the drone.

(a) Second attempt (b) Second attempt

Figure 4.12: Images from second attempt video

For the third attempt, the same propeller and battery configuration was utilized. The flight path is illustrated in Figure 4.13, which also includes the path from the previous attempt.

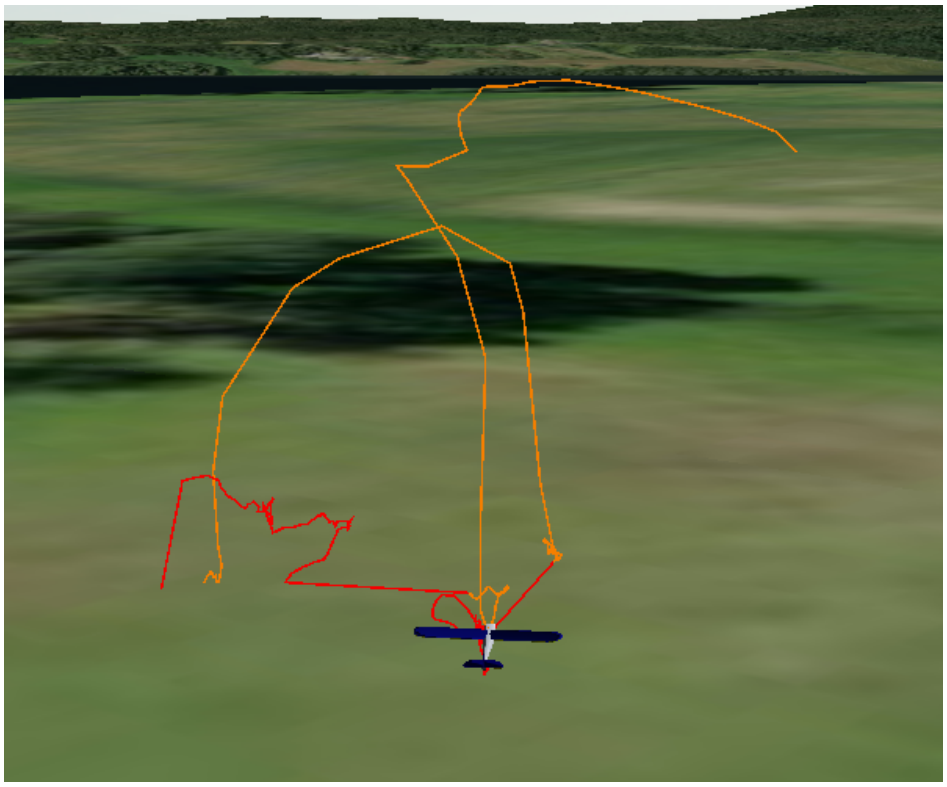

Figure 4.13: Test flight four attempt three - full path

During this test flight, the drone managed to successfully maintain stability upon launch, as can be seen from the first image in Figure 4.14d. However, shortly after the launch, the drone began rolling to the right, as depicted in the second image in the figure. Images three and four display the drone's orientation as it attempts to stabilize. Throughout the remainder of the flight, the drone remained in a stabilized orientation but gradually lost altitude due to the reduced throttle input from the pilot.

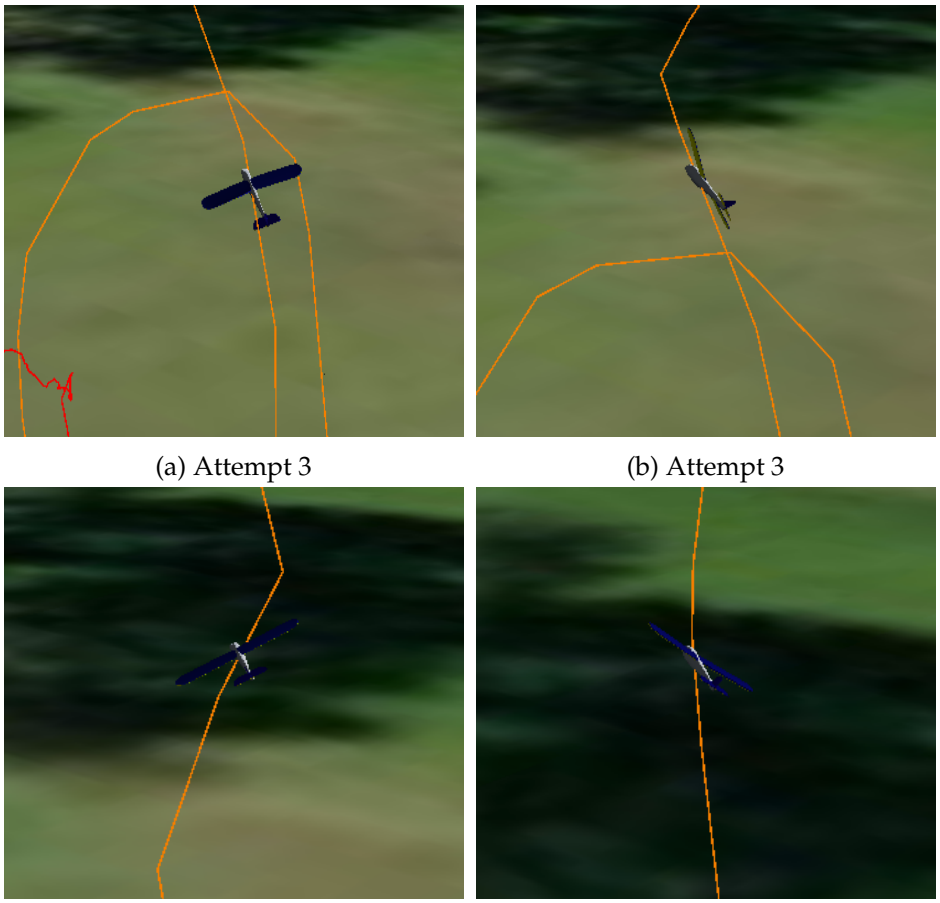

(a) Attempt 3 (b) Attempt 3

(c) Attempt 3 (d) Attempt 3

Figure 4.14: Images from video of attempt 3

Unfortunately, the terrain where the drone crashed was very dry soil, lacking the cushioning effect of the soft vegetation as in the previous landings. The drone's landing can be seen in Figure 4.15a, where the motor became lodged in the ground, and the carbon fiber rod for the tail snapped cleanly off. Further examination revealed additional damages, including another broken propeller and the right wing cover suffering some damage on the underside. The screws responsible for keeping the wing cover attached were also bent due to the impact from the crash, as shown in Figure 4.15b.

(a) Test flight four attempt three crash (b) Damage from test flight four attempt three crash

Figure 4.15: Test flight four attempt three crash

Chapter 5

Discussion

This section will analyze the results obtained throughout the different drone revisions and test flights, emphasizing the performance of the morphing mechanism, flight characteristics, and the challenges faced during the design and development process. The discussion aims to offer additional insights into the implications of the results.

5.1 Overview of the Project

The primary goal of this thesis was to design and develop a bio-inspired drone. This project's scope was narrowed down to focus on developing a morphing mechanism that could effectively reduce the drone's wing area during flight. Over two different morphing mechanisms and six revisions, significant improvements were made to the morphing mechanism, most notably being the increase of wing area and an increase in the speed of the actual morphing time.

The latest revision (revision six) had the capability of reducing the total wing area by 15.11% during flight. While this reduction of the wing area seems promising, it is essential to consider whether it is a sufficient amount of reduction in the area to impact the overall flight dynamics of the drone.

Additionally, the speed of the morphing mechanism was improved, reducing the total time necessary for a full morph from two seconds (in revision two) down to 0.5 seconds in the latest revision. This reduction in time is crucial, as a faster morph allows quicker and more efficient transitions between the different flight modes, which could result in better overall flight performance.

5.2 Prototype One

In the design phase, the initial prototype showed promise with its cogwheel-based design, which aimed to increase the structural stability of the wings while in the fully extended position. Additionally, repositioning the servos further back on the drone served the function of ensuring a more balanced weight distribution, thus contributing to a more balanced

center of gravity. However, printing the components made it apparent that the force necessary to move the bottom sliding bracket to extend the top sliding bracket was most likely more than the initial servos could provide. This issue could result from a design flaw, as the development of the second prototype began before this idea could be explored further. Another potential issue could be the minor inaccuracies that can occur in smaller 3D prints, which was another reason to explore a different morphing method.

As a result of these issues, this issue remained unverified due to the inability to install it or test it with a servo properly. Ultimately, this prototype of the morphing mechanism, as was depicted in Figure 3.3, proved unsuccessful due to the difficulties encountered in moving the cogwheel and sliding bracket connected to the main plate.

5.3 Drone body

The drone body plays a vital role in the structural integrity of the drone as it houses all the internal components and functions as the primary connection for every external component. Throughout the project, the body underwent numerous changes, and the most notable change was the material change, going from foamboard to foamboard with some PLA and lightweight PLA.

Furthermore, the transition to lightweight PLA offered a fully customized body made in Inventor to be printed without suffering the consequences of the much more significant increase in weight that PLA would have had.

The lightweight PLA did, however, bring in some undesirable characteristics. In two out of three crashes, the frontmost part of the body kept coming loose. Overall, the body quickly became the most fragile part of the drone.

5.4 Prototype Two

The following sections will explore the various components of the second morphing mechanism, focusing on the modifications. A detailed analysis of each part will be included. Following the elaboration of the parts, the outcome of the test flights will be evaluated, and the performance and functionality of the latest revision will be evaluated. This analysis will identify the project's successes and which parts should be refined to develop this design further.

5.5 Sliding Base

The sliding base provided the foundation for the sliding rack and enabled smooth movement during the morphing. Early on in the development of the morphing mechanism, it became apparent that folding the feathers onto each other became increasingly difficult as their thickness increased beyond

that of the original prototype. Due to this, the sliding base underwent several iterations to minimize friction and ensure a smoother transition between fully withdrawn and extended feathers. These changes directly impacted the morphing mechanism's overall performance.

However, due to it being made in regular PLA and having to withstand the forces extended onto each wing, the carbon fiber rod being installed was a necessary modification. Future improvements to the sliding base may include exploring alternative materials, such as utilizing carbon fiber-filled printing, where carbon fiber is infused into the material to increase the strength of the final product. Additionally, reducing the friction between the sliding base and the rack could enable a smoother morph.

5.6 Sliding Rack

The sole function of the sliding rack in the morphing mechanism is to slide smoothly in the sliding base, adjusting the position of the feathers as required. The sliding rack must be able to slide with minimal friction in order to ensure a quick morph. In the earliest versions of the sliding rack, the entirety was printed in one go, using 3D-printed pins instead of screws to attach the feathers. However, replacing the pins with screws allowed for a more structurally sound design.

The sliding rack saw a huge variety in the printing method in order to minimize the friction between the sliding rack and the sliding base, as well as the friction between the sliding rack and the feathers. As was described in Section 3.3.3, the sliding base was redesigned with elevated bases to facilitate smoother folding of the feathers. This design was mirrored for the sliding rack to elevate the corresponding feathers to enable a cooperative interplay between the two parts.

Future improvements for the sliding rack could continue to explore different designs and printing methods to further reduce the friction between all parts connected to it.

5.7 Feather

In Section 3.3.2, the initial shape and structure of the feathers were established. In order to assess their functionality, a 3D-printed prototype was created to evaluate the flexibility and strength of the design. While the idea of covering the feathers with an air-tight material was still in effect, the ideal thickness was being explored. Through trial and error, a thickness of 2.5mm was able to resist a sufficient amount of bending. However, this thickness leads to the necessity of adjusting other components to accommodate the increased size.

The final feather design, presented in the results, had a thickness of 2mm. In addition to the increased strength and more extended design, this version also featured a slated edge to allow for a smoother folding between the feathers themself.

Early in the prototyping phase, the possibility of alternating the thickness of the base of each feather was explored. However, implementing this approach proved challenging compared to elevating the bases of the sliding base and sliding rack. The main issue that presented this issue was that the feathers were only elevated at the base, not providing any support further back. Because of these challenges, implementing this change on the other components was the most convenient solution.

5.8 Test Flights

This section will take an in-depth look into the different test flights performed during this project.

5.8.1 First Test Flight

The main goal of the first test flight was to evaluate the overall performance and functionality of the drone. A thorough investigation of the flight revealed that a misaligned center of gravity likely caused the aggressive upward pitching at the start of the flight. With the battery positioned at the rear of the drone, the center of gravity was located close to the furthest back point on the feathers. Ideally, the center of gravity should be in close proximity to the center of lift, which is challenging to determine in this case due to the unconventional design of the drone. Nevertheless, an appropriate starting point is to have the center of gravity located slightly forward from the middle of the wings, as the front contributes more to the generated lift.

Although the misaligned center of gravity was a severe oversight, it served as a lesson for future iterations by highlighting the importance of implementing proper measures to prevent such oversights. The overall insight gained from this flight was invaluable, as it guided the drone's design toward an improved product and exposed several shortcomings in the pre-flight checklist.

5.8.2 Second Test Flight

The second test flight's objective was primarily to evaluate the drone's overall performance with the newly implemented modifications and to experiment with different launching methods. However, a crash during the first attempt provided an opportunity to test the performance of different propellers.

The first attempt demonstrated why conventional fixed wings are launched in an upward trajectory instead of a horizontal trajectory. The idea behind testing a horizontal launch was to observe if the drone could independently generate sufficient speed to initiate a climb. However, when the drone was launched, it quickly plummeted toward the ground as it was unable to generate enough speed on its own. Since the drone was airborne for such a short time, observing any change in flight characteristics with the newly implemented modifications was difficult.

In retrospect, this outcome was somewhat predictable, as a proper launch is crucial for initiating flight successfully. This is especially important for such an unconventional drone where the amount of lift generated is still being determined. A more traditional launching method will be utilized for future attempts to improve the chances of achieving sustained flight.

For the second attempt, the propeller was changed to that of a higher dimension. Due to the outcome of the previous flight, a traditional launching method was used, where the drone is thrown in a more upward trajectory. However, the drone started pitching aggressively upwards and started to climb excessively, which led to a stall. Shortly after stalling and losing all speed, it fell nose-first toward the ground and crashed. It is hard to pinpoint the exact cause of the stall, but it was likely a combination of inadequate pilot input, insufficient lift, and an angle of attack of 0 degrees.

For such an unconventional fixed wing, determining the proper amount of lift needed and the ideal angle of attack involves a certain degree of trial and error. Consequently, many of the factors that could have contributed to this crash are part of an iterative process of designing an unconventional fixed-wing drone with morphing wing capabilities.

5.8.3 Third Test Flight

The primary objective of the third test was to evaluate the drone's functionality after implementing several modifications assessed as potential improvements based on previous test flights. Additionally, different battery and propeller configurations were supposed to be tested. For the first attempt, the maximum thrust was increased by approximately 50% as a result of upgrading the motor and affixing an appropriate propeller. Unfortunately, the drone was unable to achieve sustained flight. As was mentioned in Section 4.3.4, the drone persisted in pitching aggressively upwards after launch, leading to a crash and irreparable damages unable to be fixed on-site.

With the increased wing area and a steeper angle of attack of 6 degrees, potential fixes for two out of three problems were implemented from the information obtained from previous flights. However, if a more experienced fixed-wing pilot had been responsible for piloting the drone, it might have been possible to recover it after it began pitching upwards. Unfortunately, an inexperienced pilot's delayed response in pitching down meant the effectiveness of the drone's control mechanism could not be verified during flight.

This flight provided the pilot with a better understanding of the drone's flight characteristics and gained insight into how the drone behaves moments into the launch. Unfortunately, the damage caused to the body due to the crash prevented further testing.

5.8.4 Fourth Test Flight

With the unfortunate outcomes of the previous flight and the unavailability of a 3D printer compatible with Lightweight PLA, it was decided to make one final attempt by printing a drone body with regular PLA. This change increased the drone's weight from 1116 grams to 1209 grams, resulting in an increase of 93 grams.

One possible explanation for the crash during the previous flight could have been the pilot's delayed reaction. Therefore, the stabilize flight mode was utilized instead of the manual mode for this attempt. Manual mode was used for test flights one and two due to the rapid adjustments of the servo. These rapid movements were mitigated when using manual mode by reducing the input weight from the controller as described in Section 3.3.13. However, with the upgraded wing cover and a steady hand from the launcher, it was decided to attempt a test flight using the stabilize flight mode to assist the pilot in stabilizing the drone after launch.

As presented in Section 4.3.5, the drone successfully achieved sustained flight and demonstrated that the morphing mechanism worked during flight. With the assistance of the stabilize flight mode, the drone could roll in both directions by reducing the wing area of the opposite side. Furthermore, the drone's orientation changing due to the morphing mechanism and effectiveness of elevators is visible in Video [32].

The second attempt resulted in a rapid attempt at an emergency landing as the drone was getting frightenedly close to the camera person. As observed in Video [34], the drone experienced some rotation due to the launching throw. However, the video also showcases how the right feathers transitioned from their resting position to fully retracting in an attempt to stabilize, causing the drone to continue rolling to the left. Additionally, the pilot tried to replicate the launch conditions of the first attempt regarding throttle input. However, the propeller change resulted in a loss of over 300 grams of thrust at maximum throttle, so the reduced thrust could have limited the drone's speed and ability to stabilize in a sufficient amount of time.

Video [33] presents a camera angle that captures the drone behaving similarly to that of an avian animal, demonstrating how the drone can quickly recover from steep roll angles. It also highlights how the stabilize flight mode requires proper tuning for this type of drone.

5.8.5 Summary of All Test Flights

A total of four test flights were conducted throughout the project to develop and design an unconventional fixed-wing drone with morphing wing capabilities. Each test flight collectively contributed to the final revision by exposing shortcomings, guiding improvement, and emphasizing the impact an iterative design process can have on the development of innovative technology, such as an unconventional fixed-wing drone with morphing wing capabilities.

Chapter 6

Conclusion

The problem statement of this thesis was to design and develop a bio-inspired drone with morphing wings capable of altering its wing area during flight. The progress of this project was documented through several revisions of the drone's design, with a series of test flights between the later revisions to evaluate the drone's performance and identify areas for improvement.

Several modifications were made to the morphing mechanism, the drone body, and the tail throughout the project's development process. The morphing mechanism evolved from a cogwheel-based design to the final sliding rack system, enabling a smoother morphing process to reduce the area of the wings more effectively. The drone body underwent several changes, both in terms of material used and significant structural changes, transitioning from the initial foamboard design to replacing certain pieces with PLA to being made entirely of lightweight PLA, allowing for more customization in the design. Despite these modifications, the development faced several challenges, such as fragility in the structural design, which resulted in multiple test flights abruptly ending due to damage caused by crashes.

The test flights conducted provided valuable insight into the drone's flight characteristics and performance, highlighting the importance of a proper launch technique, correct input from the pilot, and the need for sufficient speed to generate enough lift. The fourth test flight demonstrated that the morphing mechanism worked effectively during flight, enabling the drone to roll in both directions by reducing the wing area of the opposite side.

In conclusion, this project demonstrates the potential for a bio-inspired drone with morphing wing capabilities. Although several challenges were encountered during the development process, the progress made through an iterative design and testing process provided a foundation for future exploration and development. This technology could be advantageous for micro drones, allowing them to adapt to their environment and withstand conditions that would otherwise have rendered them useless. Future work to improve the drone's performance could include experimenting with alternative materials to increase the structural strength, optimizing the

morphing mechanism by further reducing friction, and refining the drone's aerodynamics to improve flight stability. By continuing to improve this concept, designing a drone with the desired performance, versatility, and efficiency that this thesis aimed for is achievable.

Bibliography

[1] Mujahid Abdulrahim and Rick Lind. 'Using avian morphology to enhance aircraft maneuverability'. In: *AIAA Atmospheric Flight Mechanics Conference and Exhibit*. 2006, p. 6643.

[2] Rajath Shetty et al. *DESIGN AND FABRICATION OF FIXED WING UAV FOR AIR AND UNDERWATER ENVIRONMENTS*. URL: http://www.kscst.iisc.ernet.in/spp/42_series/SPP42S/02_Exhibition_Projects/127_42S_BE_1559.pdf (visited on 27/04/2023).

[3] atom. *Radio controlled Aeromodelling*. URL: http://modelairplanelibrary.blogspot.com/p/thumb-rule-for-rc-plane-flying.html (visited on 27/04/2023).

[4] Mike Ball. *VTOL UAV Used for Fire Detection and Monitoring*. 2020. URL: https://www.unmannedsystemstechnology.com/2020/05/vtol-uav-used-for-fire-monitoring-and-location/ (visited on 13/05/2023).

[5] Balsabeavers. *Parts of an airplane*. URL: http://www.balsabeavers.com/information/articles/quiz/explanation_q2.html (visited on 10/06/2022).

[6] Aneesh N Chand, Michihiro Kawanishi and Tatsuo Narikiyo. 'Design analysis, modelling and experimental validation of a bird-like Flapping-Wing flying robot'. In: (2014).

[7] Eric Chang et al. 'Soft biohybrid morphing wings with feathers underactuated by wrist and finger motion'. In: *Science Robotics* 5.38 (2020), eaay1246.

[8] Matteo Di Luca et al. 'Bioinspired morphing wings for extended flight envelope and roll control of small drones'. In: *Interface focus* 7.1 (2017), p. 20160092.

[9] Dualsky. *ECO 2316C-V2 series brushless outrunners 2216*. URL: http://shop.dualsky.com/eco-2316c-v2-series-brushless-outrunners-2216_p0271.html (visited on 01/05/2023).

[10] Dualsky. *ECO2312C-V2 series brushless outrunners 2212*. URL: http://shop.dualsky.com/eco2312c-v2-series-brushless-outrunners-2212_p0275.html (visited on 01/05/2023).

[11] FAA. *Flight Controls*. URL: https://www.faa.gov/regulations_policies/handbooks_manuals/aviation/phak/media/08_phak_ch6.pdf (visited on 10/06/2022).

[12] FAA. *Satellite Navigation - GPS - How It Works*. URL: https://www.faa.gov/about/office_org/headquarters_offices/ato/service_units/techops/navservices/gnss/gps/howitworks (visited on 09/05/2023).

[13] filament2print. *LW-PLA*. URL: https://filament2print.com/gb/special-pla/1550-lw-pla.html#:~:text=LW%5C%2DPLA%5C%20is%5C%20a%5C%20filament,65%5C%25%5C%20by%5C%20varying%5C%20the%5C%20density. (visited on 09/05/2023).

[14] Frank E Fish et al. *The tubercles on humpback whales' flippers: application of bio-inspired technology*. 2011.

[15] John Flanagan et al. 'Development and flight testing of a morphing aircraft, the NextGen MFX-1'. In: *48th AIAA/ASME/ASCE/AHS/ASC Structures, Structural Dynamics, and Materials Conference*. 2007, p. 1707.

[16] National Museum of the united states air force. *Kettering Aerial Torpedo "Bug"*. URL: https://www.nationalmuseum.af.mil/Visit/Museum-Exhibits/Fact-Sheets/Display/Article/198095/kettering-aerial-torpedo-bug/ (visited on 10/06/2022).

[17] Jouav. *Electronic Speed Controller (ESC): Everything You Need to Know*. URL: https://www.jouav.com/blog/electronic-speed-controller-esc.html#:~:text=ESC%5C%20for%5C%20drones%5C%3F-,What%5C%20is%5C%20an%5C%20ESC%5C%20for%5C%20drones%5C%3F,and%5C%20direction%5C%20of%5C%20the%5C%20drone. (visited on 23/04/2023).

[18] Maryann Lawlor. *The Shape Of Wings To Come*. 2006. URL: https://www.afcea.org/content/shape-wings-come. (visited on 10/06/2022).

[19] Jinsong Leng et al. 'Shape-memory polymers and their composites: stimulus methods and applications'. In: *Progress in Materials Science* 56.7 (2011), pp. 1077–1135.

[20] Oscar Liang. *Flight controller explained*. URL: https://oscarliang.com/flight-controller-explained/ (visited on 23/04/2023).

[21] Oscar Liang. *What are ESC, UBEC and BEC*. URL: https://oscarliang.com/what-is-esc-ubec-bec-quadcopter/ (visited on 23/04/2023).

[22] Peter Lobner. *Festo's SmartBird and BionicSwift – A Decade of Progress in Deciphering How Birds Fly*. 2020. URL: https://lynceans.org/all-posts/festos-smartbird-and-bionicswift-a-decade-of-progress-in-deciphering-how-birds-fly/ (visited on 10/06/2022).

[23] Richard Major. *RQ-2 Pioneer: The Flawed System that Redefined US Unmanned Aviation*. Tech. rep. Air Command and Staff College Mawell AFB United States, 2012.

[24] Anna-Maria Rivas McGowan et al. 'Recent results from NASA's morphing project'. In: *Smart structures and materials 2002: industrial and commercial applications of smart structures technologies*. Vol. 4698. SPIE. 2002, pp. 97–111.

[25] Jianjun Ni et al. 'Bioinspired intelligent algorithm and its applications for mobile robot control: a survey'. In: *Computational intelligence and neuroscience* 2016 (2016), pp. 1–1.

[26] Drone Nodes. *Drone Motor Fundamentals – How Brushless Motor Works*. URL: https://dronenodes.com/drone-motors-brushless-guide/ (visited on 10/06/2022).

[27] Gary Parker and Johnny Borbone. 'Wing and gliding dynamics of a flapping winged ornithopter'. In: *2010 World Automation Congress*. IEEE. 2010, pp. 1–5.

[28] Hoang Vu Phan and Hoon Cheol Park. 'Mimicking nature's flyers: a review of insect-inspired flying robots'. In: *Current Opinion in Insect Science* 42 (2020), pp. 70–75.

[29] PX4. *mRo Pixracer*. URL: https://docs.px4.io/main/en/flight_controller/pixracer.html (visited on 13/05/2023).

[30] Roger. *A Guide to Understanding LiPo Batteries*. URL: https://rogershobbycenter.com/lipoguide (visited on 10/06/2022).

[31] K. Sekar et al. 'Aerodynamic design and structural optimization of a wing for an Unmanned Aerial Vehicle (UAV)'. In: *IOP Conference Series: Materials Science and Engineering* 764 (Mar. 2020), p. 012058. DOI: 10.1088/1757-899X/764/1/012058.

[32] *Test flight four attempt one*. 2023. URL: https://www.youtube.com/watch?v=ss56P58L7A0 (visited on 11/05/2023).

[33] *Test flight four attempt three*. 2023. URL: https://www.youtube.com/watch?v=qKZicUK2t50 (visited on 11/05/2023).

[34] *Test flight four attempt two*. 2023. URL: https://www.youtube.com/watch?v=JF15Tn-c-SY (visited on 11/05/2023).

[35] TWI. *TWI-global*. URL: https://www.twi-global.com/technical-knowledge/faqs/technology-readiness-levels#:~:text=Technology%5C%20Readiness%5C%20Level%5C%20Examples&text=Scientific%5C%20observations%5C%20made%5C%20and%5C%20reported,are%5C%20speculative%5C%20at%5C%20this%5C%20stage (visited on 10/06/2022).

[36] twi-global. *WHAT IS PLA? (EVERYTHING YOU NEED TO KNOW)*. URL: https://www.twi-global.com/technical-knowledge/faqs/what-is-pla#HowisitMade (visited on 27/04/2023).

[37] FEDERAL AVIATION ADMINISTRATION U.S. Department of Transportation. *Aircraft weight and balance handbook: 2016*. U.S. Department of Transportation, Federal Aviation Administration, Airman Testing Standards Branch, 2016.

[38] Vectornav. *WHAT IS AN INERTIAL MEASUREMENT UNIT?* URL: https://www.vectornav.com/resources/inertial-navigation-articles/what-is-an-inertial-measurement-unit-imu (visited on 27/04/2023).

[39] Chateau de Versailles. *the first hot air balloon flight*. URL: https://en.chateauversailles.fr/discover/history/key-dates/first-hot-air-balloon-flight (visited on 10/06/2022).

[40] Richard Whittle. *The Man Who Invented the Predator*. 2013. URL: https://www.smithsonianmag.com/air-space-magazine/the-man-who-invented-the-predator-3970502/ (visited on 10/06/2022).

[41] Lung-Jieh Yang et al. 'Check-valve design in enhancing aerodynamic performance of flapping wings'. In: *Applied Sciences* 11.8 (2021), p. 3416.

Appendix

Inventor files of the latest version of all components are uploaded as an appendix.